Joint Compensation of Transmitter and Receiver IQ Imbalance for MIMO-OFDM Over Doubly Selective Channels

Mojtaba Beheshti, Mohammad Javad Omidi & Ali Mohammad Doost-Hoseini

Wireless Personal Communications
An International Journal

ISSN 0929-6212
Volume 70
Number 2

Wireless Pers Commun (2013)
70:537-559
DOI 10.1007/s11277-012-0707-2

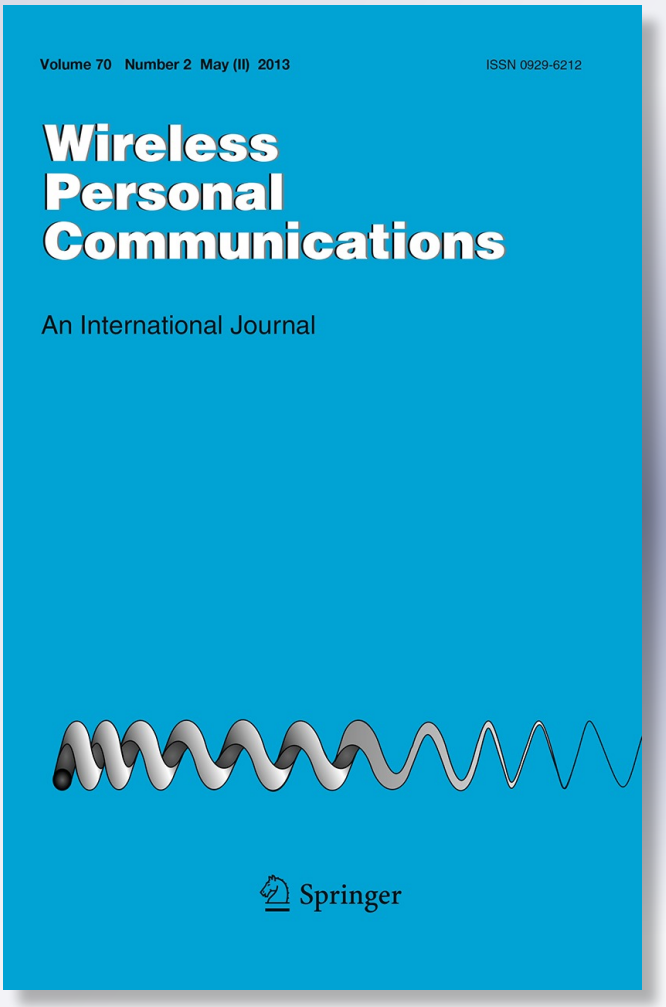

Springer

Wireless Pers Commun (2013) 70:537–559
DOI 10.1007/s11277-012-0707-2

Joint Compensation of Transmitter and Receiver IQ Imbalance for MIMO-OFDM Over Doubly Selective Channels

Mojtaba Beheshti · Mohammad Javad Omidi · Ali Mohammad Doost-Hoseini

Published online: 15 June 2012

Abstract Multiple-input multiple-output orthogonal frequency division multiplexing (MIMO-OFDM), as a viable technique, is being widely considered for high data rate and bandwidth efficient wireless communications. However, analog impairments like in-phase/quadrature (IQ) imbalance decrease the performance of this technique. Furthermore, time variations of a doubly selective channel cause intercarrier interference (ICI) which again degrades the performance. In this paper, the digital compensation of both the transmitter and the receiver IQ imbalances in MIMO-OFDM transmission over doubly selective channels is studied. In particular, basis expansion model is employed to develop a novel IQ formulation for a time-varying channel. Using this formulation, two receiver schemes are suggested to jointly mitigate the IQ imbalance and channel time variation effects. In deriving one of these schemes, the general case of an insufficient cyclic prefix (CP) for OFDM modulation is also considered. An insufficient CP results in interblock interference (IBI). The proposed approach for insufficient CP case, unifies several existing methods for IQ imbalance compensation and IBI/ICI cancellation. Simulation results show that this approach considerably improves the achievable bit-error-rate performance.

Keywords In-phase/quadrature (IQ) imbalance · Multiple-input multiple-output (MIMO) · Orthogonal frequency division multiplexing (OFDM) · Doubly selective channel · Compensation

1 Introduction

Orthogonal frequency division multiplexing (OFDM) [1] has received considerable attention in recent years [2]. It has been used in a wide range of applications including asymmetric

M. Beheshti (✉)
Information and Communication Technology Institute, Isfahan University of Technology, Esfahän, Iran
e-mail: behesht@cc.iut.ac.ir

M. J. Omidi · A. M. Doost-Hoseini
Department of Electrical and Computer Engineering, Isfahan University of Technology, Esfahän, Iran

digital subscriber line (ADSL), wireless local area networks such as IEEE 802.11 for wireless fidelity (WiFi), wireless metropolitan area networks such as IEEE 802.16 for worldwide interoperability for microwave access (WiMAX), and power-line communications (PLC). OFDM has also been considered for regional area networks using cognitive radio (CR) technology as in IEEE 802.22 and various applications involved in the third generation partnership project (3GPP) long-term evolution (LTE) [3]. The flexibility of OFDM provides opportunities to incorporate advanced techniques, such as adaptive bit loading and transmit/receive diversity, in order to improve transmission efficiency [4]. For wideband transmission, OFDM is combined with space-time coding (STC) or spatial/temporal processing to achieve higher user throughput, improved signal quality and increased system capacity. Therefore, multiple-input multiple-output OFDM (MIMO-OFDM) has attracted lot of interest in various wireless communication systems and standards [5].

A limiting factor in the practical implementation of high-speed MIMO-OFDM systems is their sensitivity to the impairments associated with analog/radio frequency (RF) processing of the signal. Examples are phase noise, non-linearities and in-phase/quadrature (IQ) imbalance. Analog impairments often stem from unpredictable fabrication variations which inevitably introduce distortions into the baseband demodulation stage. Reference [6] reviews several important impairments in the analog RF chain of transceivers. Most of these impairments cannot be entirely or efficiently compensated in the analog domain due to power-area-cost trade-offs in implementation. Hence, digital compensation techniques have been recently investigated [7,8].

This paper focuses on the effect of IQ imbalance and its compensation in the digital domain. IQ imbalance is defined as any amplitude/phase mismatch between physical analog in-phase (I) and quadrature-phase (Q) signal branches which arises from relative differences between analog components of the IQ paths [9,10]. This mismatch may be present at both the transmitter (Tx) and the receiver (Rx). At the Tx, the imperfections of the up-conversion stage, I and Q filters and digital-to-analog converters (DACs) may result in IQ imbalance. At the Rx, the down-conversion, I and Q filtering, amplification, and sampling stages may cause imbalance. Designing a high performance MIMO-OFDM receiver requires efficient digital-domain solution of the IQ imbalance.

There is an extensive literature on the performance analysis and digital compensation of IQ imbalance in single-input single-output (SISO)-OFDM systems [11–18]. The effect of the receiver IQ imbalance and the resulting performance degradation have been discussed in [11]. Reference [12] considers the down-converter IQ imperfections and suggests a compensation scheme based on adaptive frequency-domain filtering. In [13–15] the joint effects of IQ imbalance at the transmitter and receiver are investigated. The authors in [16] present a method for OFDM link capacity and bit-error-rate (BER) calculation that jointly considers various receiver imperfections such as carrier frequency offset (CFO), channel estimation error and flat receiver IQ imbalance. Reference [17] analyzes the influence of IQ imbalance in frequency selective channels and shows that the transmit IQ imbalance gives rise to diversity gains with proper receiver processing. A preamble structure for joint estimation of CFO and IQ imbalance is developed in [18].

Recently, several articles have addressed the effects of IQ imbalance in MIMO-OFDM systems and their digital compensation [19–24]. In [19,20] mathematical analysis of the influence of IQ mismatch on the performance of MIMO-OFDM systems is presented. An adaptive compensation scheme for the receiver induced IQ imbalance is developed in [21]. Reference [22] analyzes the impact of IQ mismatch and phase noise as a function of the number of antennas and derives an algorithm for joint IQ mismatch cancellation and MIMO decoding. The IQ imbalance effects in space-time coded transmit diversity system are

studied in [23] and two digital compensation methods are proposed for combating the resulting distortion. In [24] a semi-blind IQ compensation scheme based on independent component analysis is suggested.

However, the above literature does not address the IQ imbalance compensation for doubly selective (time- and frequency-selective) channels. In doubly selective (DS) channels, time variations of the channel over an OFDM block lead to loss of orthogonality between subcarriers and cause intercarrier interference (ICI). In addition, when the cyclic prefix (CP) of OFDM modulation is less than the channel delay spread, interblock interference (IBI) arises which again results in ICI. Future wireless applications that operate at high carrier-frequencies, at high levels of mobility, and at high capacities, confront DS fading. This paper is motivated by the need for efficient receiver design for such applications. The purpose of this paper is to investigate the compensation of IQ imbalance for MIMO-OFDM systems over DS channels. It is assumed that the channel varies over each OFDM block and the CP is shorter than required for the combined effects of IQ imbalance and the channel. The paper has two main contributions: (1) a closed-form input-output relation for MIMO-OFDM systems with IQ imbalance under DS fading is developed. This relation is derived using basis expansion model (BEM) [25] to describe the combined effects of IQ imbalance and channel impulse response. The relation considers the influences of frequency-dependent (FD) and frequency-independent (FI) IQ imbalances at both Tx and Rx; and (2) using the derived closed-form relation, two frequency-domain equalization approaches are proposed that jointly mitigate the interference and Tx/Rx IQ imbalance for an arbitrary CP length. The proposed approach for an insufficient CP, extends and unifies several earlier methods for IQ imbalance compensation and/or interference cancellation.

Similarly, in [26] the authors discuss the problem of IQ imbalance under DS fading and derive a mathematical framework to characterize and mitigate IQ imbalance and channel time variations due to Doppler spread. Also, [27] addresses the issue of IQ imbalance for DS channels. However, the proposed techniques in this paper are different from those proposed in [26] and [27].

- With respect to [26]:
  (a) In this paper, unlike [26], the BEM is used to describe the DS channel.
  (b) Ref. [26], like most of the previous works, chooses a CP longer than what is required for the combined effects of IQ imbalance and channel impulse response to avoid IBI. Whereas, this paper assumes an arbitrary CP length which may result in IBI.
  (c) While SISO transmission is considered in [26], this paper assumes a MIMO system.
- With respect to [27]:
  (a) The proposed approaches in this paper, compensate for joint Tx/Rx frequency-independent and frequency-dependent IQ imbalances. Whereas, in [27] merely frequency-independent IQ imbalance at the receiver is discussed.
  (b) In this paper, the equalization method is designed directly in the frequency domain. However, [27] derives a frequency-domain equalizer (FEQ) by transferring a time-domain equalizer (TEQ) to the frequency domain. Furthermore, the only interpretation expressed in [27] for FEQ is that it is the result of transferring a TEQ to the frequency domain; while, this paper presents a clear interpretation for the proposed approach.
  (c) The FEQ in [27] has different structures for different BEM resolutions (to be defined later), whereas the proposed method of this paper uses a single structure with less complexity for different values of BEM resolution.

(d) The proposed FEQ in [27] has almost the same BER performance for critically-sampled as well as over-sampled BEM. However, increasing the BEM resolution, considerably increases the BER performance of the proposed method in this paper.
(e) This paper considers MIMO systems while [27] focuses on SISO systems.

This paper is organized as follows. In Sect. 2, the system model is introduced and IQ imbalance is formulated. In Sect. 3, an IQ imbalance compensation method for transmission over a time-invariant (TI) frequency selective channel is proposed. Using the results of Sect. 3, two compensation methods for DS channel are introduced in Sect. 4. Simulation results are presented in Sect. 5, and conclusions are given in Sect. 6.

Notation Column matrices (vectors) are indicated in bold uppercase (lowercase). Superscripts T, H, and $*$ represent transpose, Hermitian and complex conjugate, respectively. $\mathcal{E}\{\cdot\}$ represents the expectation operator. The convolution and the Kronecker product are denoted by $\star$ and $\otimes$, respectively. $\boldsymbol{a}_m$ is the mth entry of vector $\boldsymbol{a}$. diag$\{\boldsymbol{a}\}$ denotes a diagonal matrix with $\boldsymbol{a}$ on the diagonal. N is the FFT/IFFT size; $\boldsymbol{\mathcal{F}}$ stands for unitary FFT matrix of size N; k is a tone index; the kth FFT row is $\boldsymbol{\mathcal{F}}^{(k)}$; c is the CP length; i is the OFDM block time index. $\boldsymbol{I}_m$ is the identity matrix of size m. $\boldsymbol{0}_{m\times p}$ is the all-zero matrix of size $m \times p$.

2 System Model and IQ Formulation

In this section, a closed-form formulation that systematically represents the input-output relation in a MIMO-OFDM system with IQ imbalance is derived. Figure 1 illustrates the system model considering both the transmitter and the receiver analog front ends. This figure shows a spatial multiplexing scheme with N_t transmit and N_r receive antennas. The input data stream is partitioned into parallel substreams and each substream is mapped into complex quadrature phase-shift keying (QPSK) symbols and arranged into OFDM blocks of length N. Each block is transformed to the time domain by the inverse fast Fourier transform (IFFT) operation and augmented by a CP of length c. The resulting blocks are then converted to analog signals and forwarded to the front-ends. The outputs of the front-ends are transmitted over the time-varying (TV) MIMO channel. At the receiver, after front-end processing and conversion to a digital format, frequency-domain IQ imbalance compensation and interference cancellation are performed to enhance the detection of the transmitted data stream.

For simplicity, the imbalance formulation is first developed for a general SISO system and then extended to the MIMO and MIMO-OFDM systems, respectively. Figure 2 depicts

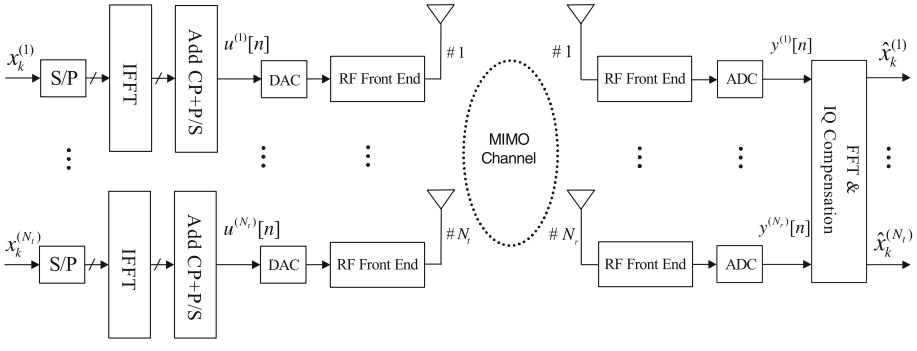

Fig. 1 MIMO-OFDM system with Tx/Rx IQ imbalance

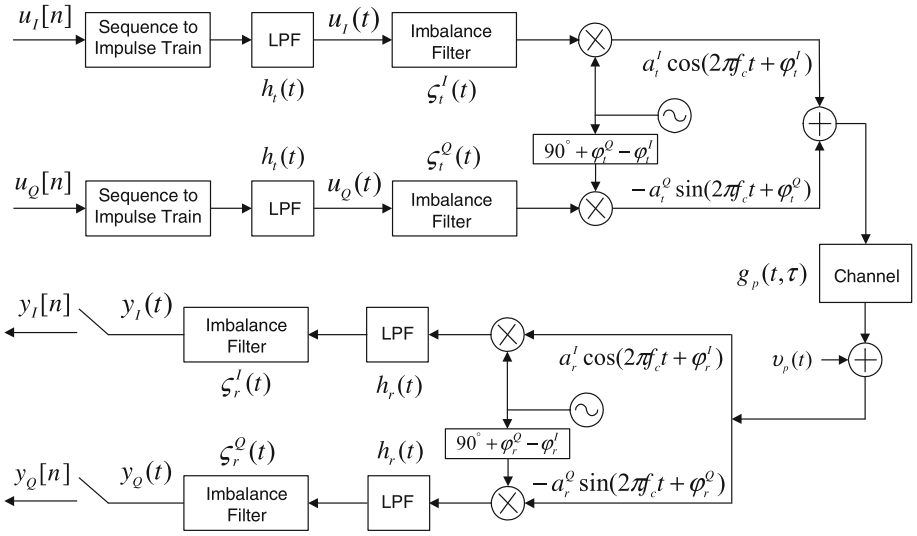

Fig. 2 IQ imbalance model for a SISO system [25]

a SISO system in which, two types of mismatches i.e, FD and FI IQ imbalances possess the following structure. The FD IQ imbalance caused by non-ideal DACs and filters in the I and Q paths of the transmitter is modeled by two imbalance filters denoted as $\zeta_t^I(t)$ and $\zeta_t^Q(t)$. The FI IQ imbalance caused by the transmitter local oscillators is characterized as amplitude mismatches a_t^I, a_t^Q and phase errors φ_t^I, φ_t^Q. Similarly, the receiver FD IQ imbalance is modeled by $\zeta_r^I(t)$ and $\zeta_r^Q(t)$. Also, the amplitude and phase mismatches of the receiver local oscillators are denoted by a_r^I, a_r^Q and φ_r^I, φ_r^Q, respectively. The receive lowpass filter (LPF) $h_r(t)$ is matched to the desired transmit LPF $h_t(t)$. If $u[n] = u_I[n] + ju_Q[n]$ denote the discrete-time complex baseband signal at the transmitter, the continuous-time ideal signal at the output of the transmit LPF is $u(t) = u_I(t) + ju_Q(t)$, where

$$u_I(t) = \sum_{n=-\infty}^{+\infty} u_I[n] h_t(t - nT)$$
$$u_Q(t) = \sum_{n=-\infty}^{+\infty} u_Q[n] h_t(t - nT) \tag{1}$$

and T is the sampling time. Using the baseband-equivalent description and following the procedure in [26], the relation between $u(t)$ and the final output signal $y(t) = y_I(t) + jy_Q(t)$ is derived as

$$\begin{aligned} y(t) = & \underbrace{\left[\lambda_r(t) \star g(t;\tau) \star \lambda_t(t) + \phi_r(t) \star g^*(t;\tau) \star \phi_t^*(t)\right]}_{\psi(t;\tau)} \star h_r(t) \star u(t) \\ & + \underbrace{\left[\lambda_r(t) \star g(t;\tau) \star \phi_t(t) + \phi_r(t) \star g^*(t;\tau) \star \lambda_t^*(t)\right]}_{\breve{\psi}(t;\tau)} \star h_r(t) \star u^*(t) \\ & + \lambda_r(t) \star h_r(t) \star \upsilon(t) + \phi_r(t) \star h_r(t) \star \upsilon^*(t) \end{aligned} \tag{2}$$

where $g(t;\tau)$ is the baseband-equivalent of the TV channel impulse response $g_p(t;\tau)$, $\upsilon(t)$ is the baseband-equivalent of complex additive white Gaussian noise (AWGN) $\upsilon_p(t)$ with zero mean and variance σ_υ^2 and

$$\begin{aligned}
\lambda_t(t) &= \frac{1}{2}\left((\mu_t+\nu_t)\,\zeta_t^I(t)+(\mu_t-\nu_t)\,\zeta_t^Q(t)\right), \quad \phi_t(t) = \frac{1}{2}\left((\mu_t+\nu_t)\,\zeta_t^I(t)-(\mu_t-\nu_t)\,\zeta_t^Q(t)\right)\\
\lambda_r(t) &= \frac{1}{2}\left(\left(\mu_r+\nu_r^*\right)\zeta_r^I(t)+\left(\mu_r-\nu_r^*\right)\zeta_r^Q(t)\right), \quad \phi_r(t) = \frac{1}{2}\left(\left(\nu_r+\mu_r^*\right)\zeta_r^I(t)+\left(\nu_r-\mu_r^*\right)\zeta_r^Q(t)\right)\\
\mu_t &= (1/2)\left(a_t^I e^{j\varphi_t^I}+a_t^Q e^{j\varphi_t^Q}\right), \qquad \nu_t = (1/2)\left(a_t^I e^{j\varphi_t^I}-a_t^Q e^{j\varphi_t^Q}\right)\\
\mu_r &= (1/2)\left(a_r^I e^{-j\varphi_r^I}+a_r^Q e^{-j\varphi_r^Q}\right), \quad \nu_r = (1/2)\left(a_r^I e^{j\varphi_r^I}-a_r^Q e^{j\varphi_r^Q}\right)
\end{aligned} \tag{3}$$

When the FI IQ imbalance is equally distributed between the I and Q branches, the imbalance is said to be symmetric [26]. The symmetric imbalance at the transmitter means that $a_t^I = 1+\tilde{\alpha}_t, a_t^Q = 1-\tilde{\alpha}_t$, $\varphi_t^I = -\varphi_t/2$ and $\varphi_t^Q = \varphi_t/2$. Thus, μ_t and ν_t in (3) are obtained as

$$\mu_t = \cos\left(\frac{\varphi_t}{2}\right) - j\tilde{\alpha}_t \sin\left(\frac{\varphi_t}{2}\right), \qquad \nu_t = \tilde{\alpha}_t \cos\left(\frac{\varphi_t}{2}\right) - j\sin\left(\frac{\varphi_t}{2}\right) \tag{4}$$

Similarly, symmetric FI imbalance at the receiver reduces the expressions for the parameters μ_r and ν_r to

$$\mu_r = \cos\left(\frac{\varphi_r}{2}\right) + j\tilde{\alpha}_r \sin\left(\frac{\varphi_r}{2}\right), \qquad \nu_r = \tilde{\alpha}_r \cos\left(\frac{\varphi_r}{2}\right) - j\sin\left(\frac{\varphi_r}{2}\right) \tag{5}$$

In the case of symmetric imbalance, the FI imbalance parameters are φ_t, φ_r, $\tilde{\alpha}_t$ and $\tilde{\alpha}_r$ where $\tilde{\alpha}$'s are usually expressed in log-scale as $\alpha_t = 10\log_{10}(1+\tilde{\alpha}_t)\,\text{dB}$ and $\alpha_r = 10\log_{10}(1+\tilde{\alpha}_r)\,\text{dB}$. Note that for symmetric FI IQ imbalance, the input-output relation (2) reduces to the FI IQ imbalance model derived in [13] for TI frequency selective channels.

Defining $\eta(t) = \lambda_r(t) \star \upsilon(t)$ and $\breve{\eta}(t) = \phi_r(t) \star \upsilon^*(t)$, (2) can be written as

$$y(t) = \psi(t;\tau) \star h_r(t) \star u(t) + \breve{\psi}(t;\tau) \star h_r(t) \star u^*(t) + \eta(t) \star h_r(t) + \breve{\eta}(t) \star h_r(t) \tag{6}$$

Equation (6) yields an equivalent model for a SISO system with IQ imbalance as depicted in Fig. 3. Note that $\psi(t;\tau)$ and $\breve{\psi}(t;\tau)$ contain the effects of both Tx/Rx IQ imbalance and the channel impulse response. So, they are denoted in this paper as combined IQ imbalance and channel (CIQCH) impulse responses. Also, it can be shown that for an ideal system with perfect IQ matching, $\psi(t;\tau)$ and $\eta(t)$ reduce to $g(t;\tau)$ and $\upsilon(t)$, respectively and the lower branch of Fig. 3 vanishes. That is, when there is no IQ imbalance, the equation (6) reduces to the conventional input-output relation.

Using (6) and assuming symbol-rate sampling, the received sequence $y[n] = y_I[n] + jy_Q[n]$ is expressed as

$$y[n] = \sum_{\theta_1=-\infty}^{+\infty} \psi[n;\theta_1]u[n-\theta_1] + \sum_{\theta_2=-\infty}^{+\infty} \breve{\psi}[n;\theta_2]u^*[n-\theta_2] + \eta[n] + \breve{\eta}[n] \tag{7}$$

where the combined response of the ideal transmit and receive filters $(h_r(t) \star h_t(t))$ is assumed to satisfy the Nyquist criterion.

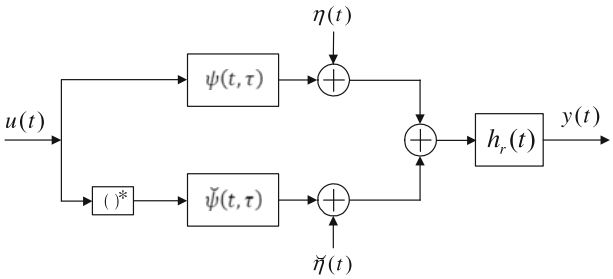

Fig. 3 Equivalent model for SISO system with IQ imbalance

To extend Eq. (7) to the MIMO case, the IQ imbalance model of Fig. 2 is used for tth transmit- rth receive path with its own imbalance parameters. Therefore,

$$y^{(r)}[n] = \sum_{t=1}^{N_t} \sum_{\theta_1=-\infty}^{+\infty} \psi^{(r,t)}[n;\theta_1]u^{(t)}[n-\theta_1] + \sum_{t=1}^{N_t} \sum_{\theta_2=-\infty}^{+\infty} \breve{\psi}^{(r,t)}[n;\theta_2]u^{(t)*}[n-\theta_2] + \eta^{(r)}[n] + \breve{\eta}^{(r)}[n] \tag{8}$$

where $y^{(r)}[n]$ is the rth received sequence; $\eta^{(r)}[n]$ and $\breve{\eta}^{(r)}[n]$ are the equivalent noise sequences corresponding the rth receive antenna and $\psi^{(r,t)}[n;\theta]$ and $\breve{\psi}^{(r,t)}[n;\theta]$ are discrete-time versions of $\psi^{(r,t)}(t;\tau)$ and $\breve{\psi}^{(r,t)}(t;\tau)$ satisfying

$$\begin{aligned} \psi^{(r,t)}[n;\theta] &= \lambda_r^{(r)}[n] \star g^{(r,t)}[n;\theta] \star \lambda_t^{(t)}[n] + \phi_r^{(r)}[n] \star g^{(r,t)*}[n;\theta] \star \phi_t^{(t)*}[n] \\ \breve{\psi}^{(r,t)}[n;\theta] &= \lambda_r^{(r)}[n] \star g^{(r,t)}[n;\theta] \star \phi_t^{(t)}[n] + \phi_r^{(r)}[n] \star g^{(r,t)*}[n;\theta] \star \lambda_t^{(t)*}[n] \end{aligned} \tag{9}$$

Finally, to extend (8) for MIMO-OFDM system, $u^{(t)}[n]$ is defined as the time-domain sequence transmitted from the tth transmit antenna which is given by

$$u^{(t)}[n] = \frac{1}{\sqrt{N}} \sum_{k=0}^{N-1} x_k^{(t)}[i] e^{j2\pi\bar{n}k/N} \tag{10}$$

where $i = \lfloor n/(N+c) \rfloor$, $\bar{n} = n - i(N+c) - c$ and $x_k^{(t)}[i]$ is the QPSK symbol transmitted on the kth subcarrier of the ith OFDM block in the tth substream. The QPSK symbols are assumed to be independent and identically distributed (i.i.d.) random variables with variance σ_s^2.

The equivalent model of Fig. 3 can be used in Fig. 1 to obtain an equivalent model for MIMO-OFDM case. In the next two sections, this model and relation (8) are employed to mitigate the IQ imbalance.

3 Imbalance Compensation over Frequency Selective Channel

In this section, a frequency-domain equalizer (FEQ) is proposed for IQ imbalance compensation when the channel is TI frequency selective. This scheme is extended to DS channels in the next section. When the communication channel between the tth transmit and the rth receive antennas, $g^{(r,t)}[n;\theta]$ is TI frequency selective, it can be represented by a finite-impulse-response (FIR) filter with constant coefficients. Moreover, assuming that the imbalance parameters $\lambda_t^{(t)}[n]$, $\phi_t^{(t)}[n]$, $\lambda_r^{(r)}[n]$ and $\phi_r^{(r)}[n]$ are TI, the CIQCH impulse responses

$\psi^{(r,t)}[n;\theta]$ and $\breve{\psi}^{(r,t)}[n;\theta]$ will also be TI and can be represented by two TI FIR filters. Hence, Eq. (8) may be rewritten as

$$\mathrm{y}^{(r)}[n] = \sum_{t=1}^{N_t}\sum_{l_1=0}^{L_1} \psi_{l_1}^{(r,t)} u^{(t)}[n-l_1] + \sum_{t=1}^{N_t}\sum_{l_2=0}^{L_2} \breve{\psi}_{l_2}^{(r,t)} u^{(t)*}[n-l_2] + \xi^{(r)}[n] \tag{11}$$

where $\psi^{(r,t)}[n;\theta]$ and $\breve{\psi}^{(r,t)}[n;\theta]$ are replaced by two FIR filters of lengthes L_1 and L_2, respectively, and $\xi^{(r)}[n] = \eta^{(r)}[n] + \breve{\eta}^{(r)}[n]$. Note that in (11) a different notation is used for the received sequence $\mathrm{y}^{(r)}[n]$ to indicate the frequency selective channel case.

In this section, it is assumed that the CP is longer than or equal to the maximum length of the CIQCH impulse responses, i.e. $c \geqslant \max(L_1, L_2)$. So, there is no IBI and the receiver can discard the multipath-corrupted CP. Using (11) and a matrix-form representation, the received sample sequence at the rth receive antenna, after CP removal, can be expressed as

$$\mathbf{y}^{(r)}[i] = \sum_{t=1}^{N_t} \boldsymbol{\Psi}^{(r,t)} \boldsymbol{P}\boldsymbol{\mathcal{F}}^H \boldsymbol{x}^{(t)}[i] + \sum_{t=1}^{N_t} \breve{\boldsymbol{\Psi}}^{(r,t)} \boldsymbol{P}\boldsymbol{\mathcal{F}}^T \boldsymbol{x}^{(t)*}[i] + \boldsymbol{\xi}^{(r)}[i] \tag{12}$$

where $\mathbf{y}^{(r)}[i] = [\mathrm{y}^{(r)}[i(N+c)+c+d+1], \ldots, \mathrm{y}^{(r)}[(i+1)(N+c)+d]]^T$, $\boldsymbol{\Psi}^{(r,t)}$ is an $N\times(N+c)$ circulant matrix with the first row $[\mathbf{0}_{1\times(c-L_1)}, \psi_{L_1}^{(r,t)}, \ldots, \psi_0^{(r,t)}, \mathbf{0}_{1\times(N-1)}]$, $\breve{\boldsymbol{\Psi}}^{(r,t)}$ is an $N\times(N+c)$ circulant matrix with the first row $[\mathbf{0}_{1\times(c-L_2)}, \breve{\psi}_{L_2}^{(r,t)}, \ldots, \breve{\psi}_0^{(r,t)}, \mathbf{0}_{1\times(N-1)}]$, $\boldsymbol{x}^{(t)}[i] = [x_0^{(t)}[i], \ldots, x_{N-1}^{(t)}[i]]^T$, $\boldsymbol{\xi}^{(r)}[i] = [\xi^{(r)}[i(N+c)+c+d+1], \ldots, \xi^{(r)}[(i+1)(N+c)+d]]^T$, d is some synchronization (decision) delay and $\boldsymbol{P}$ is the CP insertion matrix given by

$$\boldsymbol{P} = \begin{bmatrix} \mathbf{0}_{c\times(N-c)} & \boldsymbol{I}_c \\ & \boldsymbol{I}_N \end{bmatrix}$$

Taking the fast Fourier transform (FFT) of both sides of (12) yields

$$\mathbf{y}_f^{(r)}[i] = \sum_{t=1}^{N_t} \boldsymbol{\mathcal{F}}\boldsymbol{\Psi}^{(r,t)} \boldsymbol{P}\boldsymbol{\mathcal{F}}^H \boldsymbol{x}^{(t)}[i] + \sum_{t=1}^{N_t} \boldsymbol{\mathcal{F}}\breve{\boldsymbol{\Psi}}^{(r,t)} \boldsymbol{P}\boldsymbol{\mathcal{F}}^T \boldsymbol{x}^{(t)*}[i] + \boldsymbol{\xi}_f^{(r)}[i] \tag{13}$$

where $\mathbf{y}_f^{(r)}[i] = \boldsymbol{\mathcal{F}}\mathbf{y}^{(r)}[i]$ and $\boldsymbol{\xi}_f^{(r)}[i] = \boldsymbol{\mathcal{F}}\boldsymbol{\xi}^{(r)}[i]$.

Defining $\boldsymbol{\Gamma}^{(r,t)} = \boldsymbol{\mathcal{F}}\boldsymbol{\Psi}^{(r,t)}\boldsymbol{P}\boldsymbol{\mathcal{F}}^H$, $\breve{\boldsymbol{\Gamma}}^{(r,t)} = \boldsymbol{\mathcal{F}}\breve{\boldsymbol{\Psi}}^{(r,t)}\boldsymbol{P}\boldsymbol{\mathcal{F}}^H$ and $\boldsymbol{x}^{(t)\#}[i] = \boldsymbol{\mathcal{F}}\boldsymbol{\mathcal{F}}^T\boldsymbol{x}^{(t)*}[i]$, (13) is reduced to

$$\mathbf{y}_f^{(r)}[i] = \sum_{t=1}^{N_t} \boldsymbol{\Gamma}^{(r,t)} \boldsymbol{x}^{(t)}[i] + \sum_{t=1}^{N_t} \breve{\boldsymbol{\Gamma}}^{(r,t)} \boldsymbol{x}^{(t)\#}[i] + \boldsymbol{\xi}_f^{(r)}[i] \tag{14}$$

It can be shown that the matrices $\boldsymbol{\Gamma}^{(r,t)}$ and $\breve{\boldsymbol{\Gamma}}^{(r,t)}$ are diagonal and the kth element of vector $\boldsymbol{x}^{(t)\#}[i]$ is the conjugate of the $(N-k)$th element of vector $\boldsymbol{x}^{(t)}[i]$. So, the kth frequency component of the received signal at the rth receive antenna, which is the kth element of vector $\mathbf{y}_f^{(r)}[i]$, is given by

$$\begin{aligned} \mathrm{y}_{f,k}^{(r)}[i] &= \sum_{t=1}^{N_t} \boldsymbol{\Gamma}^{(r,t)}(k,k) x_k^{(t)}[i] + \sum_{t=1}^{N_t} \breve{\boldsymbol{\Gamma}}^{(r,t)}(k,k) x_{N-k}^{(t)*}[i] + \xi_{f,k}^{(r)}[i] \\ &= \boldsymbol{\gamma}_k^{(r)} \boldsymbol{x}_k[i] + \breve{\boldsymbol{\gamma}}_k^{(r)} \boldsymbol{x}_{N-k}^*[i] + \xi_{f,k}^{(r)}[i] \end{aligned} \tag{15}$$

where $\boldsymbol{\gamma}_k^{(r)} = [\boldsymbol{\Gamma}^{(r,1)}(k,k),\ldots,\boldsymbol{\Gamma}^{(r,N_t)}(k,k)]$, $\check{\boldsymbol{\gamma}}_k^{(r)} = [\check{\boldsymbol{\Gamma}}^{(r,1)}(k,k),\ldots,\check{\boldsymbol{\Gamma}}^{(r,N_t)}(k,k)]$, $\boldsymbol{x}_k[i] = [x_k^{(1)}[i],\ldots,x_k^{(N_t)}[i]]^T$, and $\boldsymbol{x}_{N-k}^*[i] = [x_{N-k}^{(1)*}[i],\ldots,x_{N-k}^{(N_t)*}[i]]^T$. Defining $\mathbf{y}_{f,k}[i] = [\mathrm{y}_{f,k}^{(1)}[i],\ldots,\mathrm{y}_{f,k}^{(N_r)}[i]]^T$, $\boldsymbol{\gamma}_k = [\boldsymbol{\gamma}_k^{(1)T},\ldots,\boldsymbol{\gamma}_k^{(N_r)T}]^T$, $\check{\boldsymbol{\gamma}}_k = [\check{\boldsymbol{\gamma}}_k^{(1)T},\ldots,\check{\boldsymbol{\gamma}}_k^{(N_r)T}]^T$, and $\boldsymbol{\xi}_{f,k}[i] = [\xi_{f,k}^{(1)}[i],\ldots,\xi_{f,k}^{(N_r)}[i]]^T$, (15) is extended to include the kth frequency components of all received signals as

$$\mathbf{y}_{f,k}[i] = \boldsymbol{\gamma}_k \boldsymbol{x}_k[i] + \check{\boldsymbol{\gamma}}_k \boldsymbol{x}_{N-k}^*[i] + \boldsymbol{\xi}_{f,k}[i] \tag{16}$$

Equation (16) means that the received signals on the kth subcarriers at all receive antennas are a linear combination of the transmitted symbols on the kth subcarriers and the conjugate of the transmitted symbols on the $(N-k)$th subcarriers at all transmit antennas. The $(N-k)$th subcarriers are known as image subcarriers. Therefore, the transmitted symbols on the kth subcarriers for $k \in \{1,\ldots,N/2-1\}$ can be estimated by linear combination of the kth and the conjugate of the $(N-k)$th frequency components of the received signals at all receive antennas as

$$\hat{\boldsymbol{x}}_k[i] = \boldsymbol{W}_1^{(k)} \mathbf{y}_{f,k}[i] + \boldsymbol{W}_2^{(k)} \mathbf{y}_{f,N-k}^*[i] \tag{17}$$

Similarly, it can be shown that the received signals on the $(N-k)$th subcarriers are a linear combination of the transmitted symbols on the $(N-k)$th subcarriers and the conjugate of the transmitted symbols on the kth subcarriers. Hence, the transmitted symbols on the $(N-k)$th subcarriers can be estimated as

$$\hat{\boldsymbol{x}}_{N-k}[i] = \boldsymbol{W}_1^{(N-k)} \mathbf{y}_{f,N-k}[i] + \boldsymbol{W}_2^{(N-k)} \mathbf{y}_{f,k}^*[i] \tag{18}$$

Defining $\tilde{\boldsymbol{x}}_k[i] = [\boldsymbol{x}_k^T[i], \boldsymbol{x}_{N-k}^H[i]]^T$ and combining (17) and (18) yields

$$\underbrace{\begin{bmatrix} \hat{\boldsymbol{x}}_k[i] \\ \hat{\boldsymbol{x}}_{N-k}^*[i] \end{bmatrix}}_{\hat{\tilde{\boldsymbol{x}}}_k[i]} = \underbrace{\begin{bmatrix} \boldsymbol{W}_1^{(k)} & \boldsymbol{W}_2^{(k)} \\ \boldsymbol{W}_2^{(N-k)*} & \boldsymbol{W}_1^{(N-k)*} \end{bmatrix}}_{\boldsymbol{W}_k^H} \underbrace{\begin{bmatrix} \mathbf{y}_{f,k}[i] \\ \mathbf{y}_{f,N-k}^*[i] \end{bmatrix}}_{\tilde{\mathbf{y}}_{f,k}[i]} \tag{19}$$

To obtain the compensation matrix $\boldsymbol{W}_k$, the following mean-square error (MSE) cost function is defined:

$$\mathcal{J}[i] = \mathcal{E}\left\{ \left\| \tilde{\boldsymbol{x}}_k[i] - \hat{\tilde{\boldsymbol{x}}}_k[i] \right\|^2 \right\} = \mathcal{E}\left\{ \left\| \tilde{\boldsymbol{x}}_k[i] - \boldsymbol{W}_k^H \tilde{\mathbf{y}}_{f,k}[i] \right\|^2 \right\} \tag{20}$$

Hence, the minimum MSE (MMSE) compensation matrix for the kth and $(N-k)$th subcarriers is given by

$$\boldsymbol{W}_{k,\mathrm{MMSE}} = \arg\min_{\boldsymbol{W}_k} \mathcal{J}[i] \tag{21}$$

Here, a relation between $\tilde{\mathbf{y}}_{f,k}[i]$ and $\tilde{\boldsymbol{x}}_k[i]$ is derived. Using (16), the $(N-k)$th frequency components of all received signals can be written as

$$\mathbf{y}_{f,N-k}[i] = \boldsymbol{\gamma}_{N-k} \boldsymbol{x}_{N-k}[i] + \check{\boldsymbol{\gamma}}_{N-k} \boldsymbol{x}_k^*[i] + \boldsymbol{\xi}_{f,N-k}[i] \tag{22}$$

Combining (16) and (22) gives

$$\tilde{\mathbf{y}}_{f,k}[i] = \underbrace{\begin{bmatrix} \boldsymbol{\gamma}_k & \check{\boldsymbol{\gamma}}_k \\ \check{\boldsymbol{\gamma}}_{N-k}^* & \boldsymbol{\gamma}_{N-k}^* \end{bmatrix}}_{\boldsymbol{\Gamma}_k} \begin{bmatrix} \boldsymbol{x}_k[i] \\ \boldsymbol{x}_{N-k}^*[i] \end{bmatrix} + \begin{bmatrix} \boldsymbol{\xi}_{f,k}[i] \\ \boldsymbol{\xi}_{f,N-k}^*[i] \end{bmatrix} = \boldsymbol{\Gamma}_k \tilde{\boldsymbol{x}}_k[i] + \boldsymbol{\mathcal{F}}_k \tilde{\boldsymbol{\xi}}[i] \tag{23}$$

where $\boldsymbol{\mathcal{F}}_k = \text{diag}\{[\boldsymbol{I}_{N_r} \otimes \boldsymbol{\mathcal{F}}^{(k)}, \boldsymbol{I}_{N_r} \otimes \boldsymbol{\mathcal{F}}^{(N-k)*}]\}$ and $\tilde{\boldsymbol{\xi}}[i] = [\boldsymbol{\xi}^{(1)\,T}[i], \ldots, \boldsymbol{\xi}^{(N_r)\,T}[i], \boldsymbol{\xi}^{(1)\,H}[i], \ldots, \boldsymbol{\xi}^{(N_r)\,H}[i]]^T$.

The solution of (21) is obtained by using (23) and solving $\partial \mathcal{J}[i]/\partial \boldsymbol{W}_k = 0$, which reduces to

$$\boldsymbol{W}_{k,\,\text{MMSE}} = \left(\boldsymbol{\Gamma}_k \boldsymbol{R}_{\tilde{\boldsymbol{x}}_k} \boldsymbol{\Gamma}_k^H + \boldsymbol{\mathcal{F}}_k \boldsymbol{R}_{\tilde{\boldsymbol{\xi}}} \boldsymbol{\mathcal{F}}_k^H\right)^{-1} \boldsymbol{\Gamma}_k \boldsymbol{R}_{\tilde{\boldsymbol{x}}_k} \tag{24}$$

where $\boldsymbol{R}_{\tilde{\boldsymbol{x}}_k} = \mathcal{E}\{\tilde{\boldsymbol{x}}_k[i]\tilde{\boldsymbol{x}}_k^H[i]\} = \sigma_s^2 \boldsymbol{I}_{(2N_t)}$ and $\boldsymbol{R}_{\tilde{\boldsymbol{\xi}}}$ is derived in the Appendix.

4 Imbalance Compensation over Doubly Selective Channel

In Sect. 3, an IQ imbalance compensation scheme for communication over TI frequency selective channels was proposed. Here, using the results of Sect. 3, IQ imbalance mitigation in doubly selective (DS) channels is addressed. When the channel between the tth transmit antenna and the rth receive antenna, $g^{(r,\,t)}[n;\theta]$ is DS, the equivalent channels $\psi^{(r,\,t)}[n;\theta]$ and $\breve{\psi}^{(r,\,t)}[n;\theta]$ will also be DS. In this paper, the well known complex-exponential basis expansion model (CE-BEM) [25,28] is used to represent $\psi^{(r,\,t)}[n;\theta]$ and $\breve{\psi}^{(r,\,t)}[n;\theta]$. In CE-BEM, the DS channel is approximated by a TV FIR filter where each tap is a superposition of complex exponential basis functions with a pre-specified frequency resolution. Using this model, the discrete-time approximations of $\psi^{(r,\,t)}[n;\theta]$ and $\breve{\psi}^{(r,\,t)}[n;\theta]$ for $n \in \{i(N+c)+c+d-L'+1, \ldots, (i+1)(N+c)+d\}$ are expressed as follows

$$\begin{aligned}
\psi^{(r,\,t)}[n;\theta] &= \sum_{l=0}^{L_1} \delta[\theta - l] \sum_{q=-Q/2}^{Q/2} h_{q,\,l}^{(r)}[i] e^{j2\pi qn/K} \\
\breve{\psi}^{(r,\,t)}[n;\theta] &= \sum_{l=0}^{L_2} \delta[\theta - l] \sum_{q=-Q/2}^{Q/2} \breve{h}_{q,\,l}^{(r)}[i] e^{j2\pi qn/K}
\end{aligned} \tag{25}$$

where L' is set to be 0 when a sufficient CP is used. In the case of insufficient CP, $L' \geqslant \max(L_1, L_2)$. The parameter Q is the number of TV basis functions. K is the BEM resolution and it is assumed to be an integer multiple of the FFT size, i.e., $K = PN$, where P is an integer greater than or equal to 1. The coefficients $h_{q,\,l}^{(r)}[i]$ and $\breve{h}_{q,\,l}^{(r)}[i]$ are kept invariant over a period of length $(N+L')T$. Substituting (25) in (8) yields

$$\begin{aligned}
y^{(r)}[n] = &\sum_{t=1}^{N_t} \sum_{l_1=0}^{L_1} \sum_{q_1=-Q/2}^{Q/2} e^{j2\pi q_1 n/K} h_{q_1,\,l_1}^{(r)}[i] u^{(t)}[n-l_1] \\
&+ \sum_{t=1}^{N_t} \sum_{l_2=0}^{L_2} \sum_{q_2=-Q/2}^{Q/2} e^{j2\pi q_2 n/K} \breve{h}_{q_2,\,l_2}^{(r)}[i] u^{(t)*}[n-l_2] + \eta^{(r)}[n] + \breve{\eta}^{(r)}[n]
\end{aligned} \tag{26}$$

In the following, Eq. (26) is employed to derive two IQ imbalance compensation methods for transmission over DS channels, when either sufficient or insufficient CP is used.

4.1 Sufficient Cyclic Prefix

In this subsection, it is assumed that the CIQCH impulse responses $\psi^{(r,\,t)}[n;\theta]$ and $\breve{\psi}^{(r,\,t)}[n;\theta]$ fit within the CP. Therefore, only IQ imbalance and ICI caused by time variations of the channel are present. As shown in Sect. 3, the effect of IQ imbalance in MIMO-OFDM

transmission over a TI frequency selective channel is that the received signals at the kth subcarriers of all receive antennas are a mixture of the transmitted signals on the kth subcarriers and image signals from $(N-k)$th subcarriers at all transmit antennas. Based on this fact, an FEQ has been proposed in Sect. 3, in which, a linear combination of the kth and $(N-k)$th subcarriers is used to estimate the transmitted symbols on these subcarriers. However, in DS channels, channel time variations cause ICI and hence, the simple linear combination in (17) cannot be directly applied. In this paper, it is proposed to remove the ICI power from each subcarrier before using the Eq. (17). In other words, one should obtain ICI-free estimates of the signals corresponding the kth and $(N-k)$th subcarriers. On the other hand, it has been observed that most of the ICI power on each subcarrier comes from a few neighboring subcarriers [29]. Hence, the so-called ICI-free estimate can be obtained using a linear combination of the FFT output samples on each subcarrier and its adjacent neighbors. Based on ICI-free estimates, (17) and (18) can be rewritten as

$$\hat{\boldsymbol{x}}_k[i] = \boldsymbol{W}_1^{(k)}[i]\hat{\boldsymbol{y}}_{f,k}[i] + \boldsymbol{W}_2^{(k)}[i]\hat{\boldsymbol{y}}_{f,N-k}^*[i] \tag{27a}$$

$$\hat{\boldsymbol{x}}_{N-k}[i] = \boldsymbol{W}_1^{(N-k)}[i]\hat{\boldsymbol{y}}_{f,N-k}[i] + \boldsymbol{W}_2^{(N-k)}[i]\hat{\boldsymbol{y}}_{f,k}^*[i] \tag{27b}$$

where $\hat{\boldsymbol{y}}_{f,k}[i] = \left[\hat{y}_{f,k}^{(1)}[i], \ldots, \hat{y}_{f,k}^{(N_r)}[i]\right]^T$ and $\hat{y}_{f,k}^{(r)}[i]$ is an ICI-free estimate of the kth frequency component of the rth received signal. Note that unlike (17), the coefficients of the linear combination in (27a,b) are assumed to be time-varying. This assumption is necessary to cope with the time-selectivity of the DS channel.

Considering Q' neighbors, the ICI-free estimate for the kth subcarrier on the rth receive antenna is expressed as follows:

$$\hat{y}_{f,k}^{(r)}[i] = \sum_{q'=-Q'/2}^{Q'/2} \alpha_{q'}^{(r,k)}[i] y_{f,k+q'}^{(r)}[i] = \sum_{q'=-Q'/2}^{Q'/2} \alpha_{q'}^{(r,k)}[i] \left(\boldsymbol{\mathcal{F}}^{(k+q')} \boldsymbol{y}^{(r)}[i]\right) \tag{28}$$

where $y_{f,k+q'}^{(r)}[i]$ is the $(k+q')$th frequency component of the received signal at the rth receive antenna, $\boldsymbol{y}^{(r)}[i] = [y^{(r)}[i(N+c)+c+d+1], \ldots, y^{(r)}[(i+1)(N+c)+d]]^T$ and $y^{(r)}[n]$ is defined in (26). Defining $\boldsymbol{\alpha}_1^{(r,k)}[i] = [\alpha_{-Q'/2}^{(r,k)}[i], \ldots, \alpha_{Q'/2}^{(r,k)}[i]]^T$ and $\boldsymbol{F}^{(k)} = \left[\boldsymbol{\mathcal{F}}^{(k-Q'/2)T}, \ldots, \boldsymbol{\mathcal{F}}^{(k+Q'/2)T}\right]^T$, (27a,b) is reduced to

$$\hat{y}_{f,k}^{(r)}[i] = \boldsymbol{\alpha}_1^{(r,k)\,T}[i] \boldsymbol{F}^{(k)} \boldsymbol{y}^{(r)}[i] \tag{29}$$

Considering (29) for different values of r and k and substituting in (27a,b) results in

$$\hat{\boldsymbol{x}}_k[i] = \boldsymbol{V}_1^{(k)}[i] \left(\boldsymbol{I}_{N_r} \otimes \boldsymbol{F}^{(k)}\right) \boldsymbol{y}[i] + \boldsymbol{V}_2^{(k)}[i] \left(\boldsymbol{I}_{N_r} \otimes \boldsymbol{F}^{(N-k)*}\right) \boldsymbol{y}^*[i] \tag{30a}$$

$$\hat{\boldsymbol{x}}_{N-k}[i] = \boldsymbol{V}_1^{(N-k)}[i] \left(\boldsymbol{I}_{N_r} \otimes \boldsymbol{F}^{(N-k)}\right) \boldsymbol{y}[i] + \boldsymbol{V}_2^{(N-k)}[i] \left(\boldsymbol{I}_{N_r} \otimes \boldsymbol{F}^{(k)*}\right) \boldsymbol{y}^*[i] \tag{30b}$$

where $\boldsymbol{y}[i] = [\boldsymbol{y}^{(1)\,T}[i], \ldots, \boldsymbol{y}^{(N_r)\,T}[i]]^T$, $\boldsymbol{V}_1^{(k)}[i] = \boldsymbol{W}_1^{(k)}[i] \times \mathrm{diag}\{[\boldsymbol{\alpha}_1^{(1,k)\,T}[i], \ldots, \boldsymbol{\alpha}_1^{(N_r,k)\,T}[i]]\}$, $\boldsymbol{V}_2^{(N-k)}[i] = \boldsymbol{W}_2^{(N-k)}[i] \times \mathrm{diag}\{[\boldsymbol{\alpha}_1^{(1,k)\,H}[i], \ldots, \boldsymbol{\alpha}_1^{(N_r,k)\,H}[i]]\}$, and $\boldsymbol{V}_1^{(N-k)}[i]$ and $\boldsymbol{V}_2^{(k)}[i]$ are defined similarly.

Combining (30a) and (30b) yields

$$\underbrace{\begin{bmatrix}\hat{\boldsymbol{x}}_k[i]\\ \hat{\boldsymbol{x}}^*_{N-k}[i]\end{bmatrix}}_{\hat{\tilde{\boldsymbol{x}}}_k[i]} = \underbrace{\begin{bmatrix}\boldsymbol{V}_1^{(k)}[i] & \boldsymbol{V}_2^{(k)}[i]\\ \boldsymbol{V}_2^{(N-k)*}[i] & \boldsymbol{V}_1^{(N-k)*}[i]\end{bmatrix}}_{\boldsymbol{V}_k^H[i]} \underbrace{\begin{bmatrix}\boldsymbol{I}_{N_r}\otimes\boldsymbol{F}^{(k)} & 0\\ 0 & \boldsymbol{I}_{N_r}\otimes\boldsymbol{F}^{(N-k)*}\end{bmatrix}}_{\boldsymbol{F}_k} \underbrace{\begin{bmatrix}\boldsymbol{y}[i]\\ \boldsymbol{y}^*[i]\end{bmatrix}}_{\tilde{\boldsymbol{y}}[i]} \tag{31}$$

Finally, the compensation matrix $\boldsymbol{V}_k[i]$ for $k \in \{1,\ldots,N/2-1\}$ is the solution of the following MMSE design criterion:

$$\boldsymbol{V}_{k,\,\mathrm{MMSE}}[i] = \arg\min_{\boldsymbol{V}_k[i]} \mathcal{E}\left\{\left\|\tilde{\boldsymbol{x}}_k[i] - \boldsymbol{V}_k^H[i]\boldsymbol{F}_k\tilde{\boldsymbol{y}}[i]\right\|^2\right\} \tag{32}$$

To solve (32), $\tilde{\boldsymbol{y}}[i]$ should be expressed in terms of transmitted symbols. Using (26), a block of N samples of the received signal at the rth receive antenna after removing the CP is shown as

$$\boldsymbol{y}^{(r)}[i] = \sum_{t=1}^{N_t}\underbrace{\sum_{q_1=-Q/2}^{Q/2}\boldsymbol{D}_{q_1}[i]\boldsymbol{\mathcal{H}}_{q_1}^{(r,t)}[i]\boldsymbol{P}\boldsymbol{\mathcal{F}}^H}_{\boldsymbol{\mathcal{G}}^{(r,t)}[i]}\boldsymbol{x}^{(t)}[i] + \sum_{t=1}^{N_t}\underbrace{\sum_{q_2=-Q/2}^{Q/2}\boldsymbol{D}_{q_2}[i]\check{\boldsymbol{\mathcal{H}}}_{q_2}^{(r,t)}[i]\boldsymbol{P}\boldsymbol{\mathcal{F}}^T}_{\check{\boldsymbol{\mathcal{G}}}^{(r,t)}[i]}\boldsymbol{x}^{(t)*}[i] + \boldsymbol{\xi}^{(r)}[i] \tag{33}$$

where $\boldsymbol{D}_{q_1}[i] = \mathrm{diag}\{\,[e^{j2\pi q_1(i(N+c)+c+d+1)/K},\ldots,e^{j2\pi q_1((i+1)(N+c)+d)/K}]\,\}$, $\boldsymbol{\mathcal{H}}_{q_1}^{(r,t)}[i]$ is an $N\times(N+c)$ circulant matrix with the first row $[\boldsymbol{0}_{1\times(c-L_1)}, h_{q_1,L_1}^{(r,t)}[i],\ldots,h_{q_1,0}^{(r,t)}[i], \boldsymbol{0}_{1\times(N-1)}]$, and the first column $[h_{q_1,L_1}^{(r,t)}[i], \boldsymbol{0}_{1\times(N-1)}]^T$, $\boldsymbol{D}_{q_2}[i]$ and $\check{\boldsymbol{\mathcal{H}}}_{q_2}^{(r,t)}[i]$ are defined similarly and other parameters are defined as in (12).

Defining $\boldsymbol{\mathcal{G}}_T^{(r)}[i] = \left[\boldsymbol{\mathcal{G}}^{(r,1)}[i],\ldots,\boldsymbol{\mathcal{G}}^{(r,N_t)}[i]\right]$, $\boldsymbol{\mathcal{G}}[i] = \left[\boldsymbol{\mathcal{G}}_T^{(1)\,T}[i],\ldots,\boldsymbol{\mathcal{G}}_T^{(N_r)\,T}[i]\right]^T$, $\check{\boldsymbol{\mathcal{G}}}_T^{(r)}[i] = \left[\check{\boldsymbol{\mathcal{G}}}^{(r,1)}[i],\ldots,\check{\boldsymbol{\mathcal{G}}}^{(r,N_t)}[i]\right]$, $\check{\boldsymbol{\mathcal{G}}}[i] = \left[\check{\boldsymbol{\mathcal{G}}}_T^{(1)\,T}[i],\ldots,\check{\boldsymbol{\mathcal{G}}}_T^{(N_r)\,T}[i]\right]^T$, $\boldsymbol{x}[i] = [\boldsymbol{x}^{(1)\,T}[i],\ldots,\boldsymbol{x}^{(N_t)\,T}[i]]^T$, and $\boldsymbol{\xi}[i] = [\boldsymbol{\xi}^{(1)\,T}[i],\ldots,\boldsymbol{\xi}^{(N_r)\,T}[i]]^T$, and using (33), the received blocks at all receive antennas are expressed as

$$\boldsymbol{y}[i] = \boldsymbol{\mathcal{G}}[i]\boldsymbol{x}[i] + \check{\boldsymbol{\mathcal{G}}}[i]\boldsymbol{x}^*[i] + \boldsymbol{\xi}[i] \tag{34}$$

Hence,

$$\tilde{\boldsymbol{y}}[i] = \begin{bmatrix}\boldsymbol{y}[i]\\ \boldsymbol{y}^*[i]\end{bmatrix} = \underbrace{\begin{bmatrix}\boldsymbol{\mathcal{G}}[i] & \check{\boldsymbol{\mathcal{G}}}[i]\\ \check{\boldsymbol{\mathcal{G}}}[i]^* & \boldsymbol{\mathcal{G}}[i]^*\end{bmatrix}}_{\tilde{\boldsymbol{\mathcal{G}}}[i]} \underbrace{\begin{bmatrix}\boldsymbol{x}[i]\\ \boldsymbol{x}^*[i]\end{bmatrix}}_{\tilde{\boldsymbol{x}}[i]} + \underbrace{\begin{bmatrix}\boldsymbol{\xi}[i]\\ \boldsymbol{\xi}^*[i]\end{bmatrix}}_{\tilde{\boldsymbol{\xi}}[i]} \tag{35}$$

Using (35), the solution of (32) is given by

$$\boldsymbol{V}_{k,\,\mathrm{MMSE}}[i] = \left(\boldsymbol{F}_k(\tilde{\boldsymbol{\mathcal{G}}}[i]\boldsymbol{R}_{\tilde{\boldsymbol{x}}}\tilde{\boldsymbol{\mathcal{G}}}^H[i] + \boldsymbol{R}_{\tilde{\boldsymbol{\xi}}})\boldsymbol{F}_k^H\right)^{-1}\boldsymbol{F}_k\tilde{\boldsymbol{\mathcal{G}}}[i]\boldsymbol{R}_{\tilde{\boldsymbol{x}}}\boldsymbol{E}^{(k)\,T} \tag{36}$$

where $\boldsymbol{R}_{\tilde{x}} = \sigma_s^2\boldsymbol{I}_{(2N_tN)}$, $\boldsymbol{R}_{\tilde{\xi}}$ is derived in the Appendix and $\boldsymbol{E}^{(k)} = \mathrm{diag}\{[\boldsymbol{I}_{N_t}\otimes\boldsymbol{e}^{(k)\,T}, \boldsymbol{I}_{N_t}\otimes\boldsymbol{e}^{(N-k)\,T}]\}$ where $\boldsymbol{e}^{(k)}$ and $\boldsymbol{e}^{(N-k)}$ are the $N\times 1$ unit vectors with a 1 in the positions k and $N-k$, respectively.

Figure 4 shows the derived equalization and IQ imbalance compensation scheme (denoted by EQCS1) for the kth subcarrier on the ath transmit antenna.

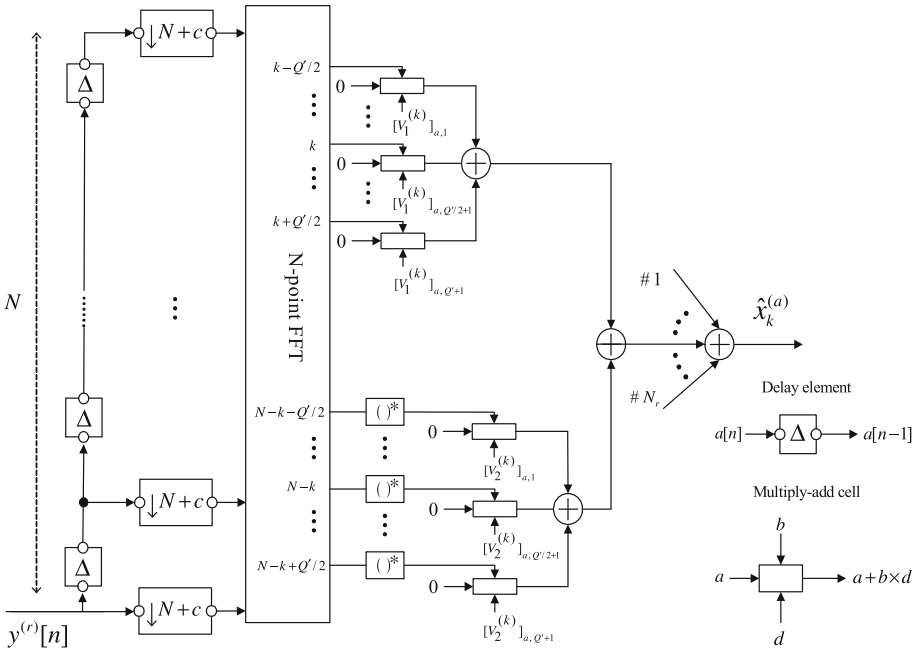

Fig. 4 Proposed equalization and IQ imbalance compensation scheme for sufficient CP (EQCS1)

4.2 Insufficient Cyclic Prefix

In this subsection, it is assumed that the CP length is shorter than the maximum length of the CIQCH impulse responses. Therefore, both IBI and ICI in addition to IQ imbalance are present. Here, the results of the previous sections are extended to jointly mitigate the IQ imbalance and IBI/ICI. In the presence of both IQ imbalance and IBI/ICI, the simple linear combination in (17) is inadequate to estimate the transmitted symbols and compensate for the IQ imbalance. In Sect. 4.1, it was proposed to modify (17) by replacing the frequency components of the kth and $(N-k)$th subcarriers with their ICI-free estimates as in (27a,b). The ICI-free estimates were derived using a linear combination of each subcarrier and its adjacent neighbors as in (28). However, when IBI is also present, each frequency component includes some IBI power and hence, equation (28) will not lead to a proper estimate of the kth frequency component. In this paper, it is suggested to modify this equation by using IBI-free estimate of each frequency component as

$$\hat{\hat{y}}^{(r)}_{f,k}[i] = \sum_{q'=-Q'/2}^{Q'/2} \alpha^{(r,k)}_{q'}[i]\,\hat{y}^{(r)}_{f,k+q'}[i] \tag{37}$$

where $\hat{y}^{(r)}_{f,k+q'}$ is an IBI-free estimate of the $y^{(r)}_{f,k+q'}$. To remove IBI from $y^{(r)}_{f,k+q'}$, this paper proposes to apply a linear combination on the $L'+1$ samples of the FFT output corresponding to the $(k+q')$th subcarrier where $L' \geqslant \max(L_1, L_2)$. These samples are provided through performing a sliding FFT on the $N+L'$ received samples of each received signal path. The sliding FFT is equivalent to $L'+1$ FFTs of size N. Substituting the supposedly IBI-free estimate $\hat{y}^{(r)}_{f,k+q'}$ in (37) yields

$$\hat{\hat{y}}_{f,k}^{(r)}[i] = \sum_{q'=-Q'/2}^{Q'/2} \alpha_{q'}^{(r,k)}[i] \left\{ \boldsymbol{\varrho}_{q'}^{(r,k)\,T}[i] \left(\tilde{\boldsymbol{\mathcal{F}}}^{(k+q')} \boldsymbol{y}'^{(r)}[i] \right) \right\} \tag{38}$$

where $\boldsymbol{\varrho}_{q'}^{(r,k)}[i]$ is a vector of length $L'+1$ which contains the coefficients of the linear combination,

$$\tilde{\boldsymbol{\mathcal{F}}}^{(k)} = \begin{bmatrix} 0 & \dots & 0 & \boldsymbol{\mathcal{F}}^{(k)} \\ \vdots & 0 & \boldsymbol{\mathcal{F}}^{(k)} & 0 \\ 0 & \iddots & 0 & \vdots \\ \boldsymbol{\mathcal{F}}^{(k)} & 0 & \dots & 0 \end{bmatrix}$$

which represents a sliding FFT operation; $\boldsymbol{y}'^{(r)}[i] = [y^{(r)}[i(N+c)+c+d-L'+1], \dots, y^{(r)}[(i+1)(N+c)+d]]^T$ and $y^{(r)}[n]$ is defined in (26). Defining $\boldsymbol{\beta}_1^{(r,k)}[i] = [\alpha_{-Q'/2}^{(r,k)}[i]\boldsymbol{\varrho}_{-Q'/2}^{(r,k)\,T}[i], \dots, \alpha_{Q'/2}^{(r,k)}[i]\boldsymbol{\varrho}_{Q'/2}^{(r,k)\,T}[i]]^T$, and $\tilde{\boldsymbol{F}}^{(k)} = [\tilde{\boldsymbol{\mathcal{F}}}^{(k-Q'/2)T}, \dots, \tilde{\boldsymbol{\mathcal{F}}}^{(k+Q'/2)T}]^T$, (38) can be rewritten as

$$\hat{\hat{y}}_{f,k}^{(r)}[i] = \boldsymbol{\beta}_1^{(r,k)\,T}[i] \tilde{\boldsymbol{F}}^{(k)} \boldsymbol{y}'^{(r)}[i] \tag{39}$$

Considering (39) for different values of r and k and substituting in (27a,b) results in

$$\hat{\boldsymbol{x}}_k[i] = \boldsymbol{U}_1^{(k)}[i] \left(\boldsymbol{I}_{N_r} \otimes \tilde{\boldsymbol{F}}^{(k)} \right) \boldsymbol{y}'[i] + \boldsymbol{U}_2^{(k)}[i] \left(\boldsymbol{I}_{N_r} \otimes \tilde{\boldsymbol{F}}^{(N-k)*} \right) \boldsymbol{y}'^{*}[i] \tag{40a}$$

$$\hat{\boldsymbol{x}}_{N-k}[i] = \boldsymbol{U}_1^{(N-k)}[i] \left(\boldsymbol{I}_{N_r} \otimes \tilde{\boldsymbol{F}}^{(N-k)} \right) \boldsymbol{y}'[i] + \boldsymbol{U}_2^{(N-k)}[i] \left(\boldsymbol{I}_{N_r} \otimes \tilde{\boldsymbol{F}}^{(k)*} \right) \boldsymbol{y}'^{*}[i] \tag{40b}$$

where $\boldsymbol{y}'[i] = [\boldsymbol{y}'^{(1)\,T}[i], \dots, \boldsymbol{y}'^{(N_r)\,T}[i]]^T$, $\boldsymbol{U}_1^{(k)}[i] = \boldsymbol{W}_1^{(k)}[i] \times \mathrm{diag}\{[\boldsymbol{\beta}_1^{(1,k)\,T}[i], \dots, \boldsymbol{\beta}_1^{(N_r,k)\,T}[i]]\}$, $\boldsymbol{U}_2^{(N-k)}[i] = \boldsymbol{W}_2^{(N-k)}[i] \times \mathrm{diag}\{[\boldsymbol{\beta}_1^{(1,k)\,H}[i], \dots, \boldsymbol{\beta}_1^{(N_r,k)\,H}[i]]\}$, and $\boldsymbol{U}_1^{(N-k)}[i]$ and $\boldsymbol{U}_2^{(k)}[i]$ are defined similarly.

Combining (40a) and (40b) yields

$$\underbrace{\begin{bmatrix} \hat{\boldsymbol{x}}_k[i] \\ \hat{\boldsymbol{x}}_{N-k}^{*}[i] \end{bmatrix}}_{\hat{\tilde{\boldsymbol{x}}}_k[i]} = \underbrace{\begin{bmatrix} \boldsymbol{U}_1^{(k)}[i] & \boldsymbol{U}_2^{(k)}[i] \\ \boldsymbol{U}_2^{(N-k)*}[i] & \boldsymbol{U}_1^{(N-k)*}[i] \end{bmatrix}}_{\boldsymbol{U}_k^H[i]} \underbrace{\begin{bmatrix} \boldsymbol{I}_{N_r} \otimes \tilde{\boldsymbol{F}}^{(k)} & 0 \\ 0 & \boldsymbol{I}_{N_r} \otimes \tilde{\boldsymbol{F}}^{(N-k)*} \end{bmatrix}}_{\tilde{\boldsymbol{F}}_k} \underbrace{\begin{bmatrix} \boldsymbol{y}'[i] \\ \boldsymbol{y}'^{*}[i] \end{bmatrix}}_{\tilde{\boldsymbol{y}}'[i]} \tag{41}$$

The following MMSE design criterion is considered to design the equalization matrix $\boldsymbol{U}_k[i]$:

$$\boldsymbol{U}_{k,\,\mathrm{MMSE}}[i] = \underset{\boldsymbol{U}_k[i]}{\arg\min}\ \mathcal{E}\left\{ \left\| \tilde{\boldsymbol{x}}_k[i] - \boldsymbol{U}_k^H[i] \tilde{\boldsymbol{F}}_k \tilde{\boldsymbol{y}}'[i] \right\|^2 \right\}, \qquad k \in \{1, \dots, N/2-1\} \tag{42}$$

Using (26), a block of $N + L'$ samples of the rth received signal is given by

$$\boldsymbol{y}'^{(r)}[i] = \sum_{t=1}^{N_t} \underbrace{\sum_{q_1=-Q/2}^{Q/2} \boldsymbol{\Omega}_{q_1}[i] \left[\boldsymbol{O}_1, \boldsymbol{H}_{q_1}^{(r,t)}[i], \boldsymbol{O}_2\right] (\boldsymbol{I}_3 \otimes \boldsymbol{P})(\boldsymbol{I}_3 \otimes \boldsymbol{\mathcal{F}}^H)}_{\boldsymbol{G}^{(r,t)}[i]} \times \tilde{\boldsymbol{x}}^{(t)}$$
$$+ \sum_{t=1}^{N_t} \underbrace{\sum_{q_2=-Q/2}^{Q/2} \boldsymbol{\Omega}_{q_2}[i] \left[\check{\boldsymbol{O}}_1, \check{\boldsymbol{H}}_{q_2}^{(r,t)}[i], \boldsymbol{O}_2\right] (\boldsymbol{I}_3 \otimes \boldsymbol{P})(\boldsymbol{I}_3 \otimes \boldsymbol{\mathcal{F}}^H)}_{\check{\boldsymbol{G}}^{(r,t)}[i]} \times \tilde{\boldsymbol{x}}^{(t)*} + \boldsymbol{\xi}'^{(r)}[i] \tag{43}$$

where $\boldsymbol{\Omega}_q[i] = \text{diag}\{[e^{j2\pi q(i(N+c)+c-L'+d+1)/K}, \ldots, e^{j2\pi q((i+1)(N+c)+d)/K}]\}$, $\boldsymbol{O}_1 = \boldsymbol{0}_{(N+L')\times(N+2c+d-L_1-L')}$, $\check{\boldsymbol{O}}_1 = \boldsymbol{0}_{(N+L')\times(N+2c+d-L_2-L')}$, $\boldsymbol{O}_2 = \boldsymbol{0}_{(N+L')\times(N+c-d)}$, $\boldsymbol{H}_{q_1}^{(r,t)}[i]$ is an $(N + L') \times (N + L_1 + L')$ Toeplitz matrix with the first column $[h_{q_1,L_1}^{(r,t)}[i], \boldsymbol{0}_{1\times(N+L'-1)}]^T$ and the first row $[h_{q_1,L_1}^{(r,t)}[i], \ldots, h_{q_1,0}^{(r,t)}[i], \boldsymbol{0}_{1\times(N+L'-1)}]$, $\check{\boldsymbol{H}}_{q_2}^{(r,t)}[i]$ is an $(N+L')\times(N+L_2+L')$ Toeplitz matrix with the first column $[\check{h}_{q_2,L_2}^{(r,t)}[i], \boldsymbol{0}_{1\times(N+L'-1)}]^T$ and the first row $[\check{h}_{q_2,L_2}^{(r,t)}[i], \ldots, \check{h}_{q_2,0}^{(r,t)}[i], \boldsymbol{0}_{1\times(N+L'-1)}]$, $\tilde{\boldsymbol{x}}^{(t)} = [\boldsymbol{x}^{(t)T}[i-1], \boldsymbol{x}^{(t)T}[i], \boldsymbol{x}^{(t)T}[i+1]]^T$ and $\boldsymbol{\xi}'^{(r)}[i] = [\xi^{(r)}[i(N+c)+c+d-L'+1], \ldots, \xi^{(r)}[(i+1)(N+c)+d]]^T$.

Defining $\boldsymbol{y}'[i] = [\boldsymbol{y}'^{(1)T}[i], \ldots, \boldsymbol{y}'^{(N_r)T}[i]]^T$, $\boldsymbol{G}_T^{(r)}[i] = \left[\boldsymbol{G}^{(r,1)}[i], \ldots, \boldsymbol{G}^{(r,N_t)}[i]\right]$, $\boldsymbol{G}[i] = \left[\boldsymbol{G}_T^{(1)T}[i], \ldots, \boldsymbol{G}_T^{(N_r)T}[i]\right]^T$, $\check{\boldsymbol{G}}_T^{(r)}[i] = \left[\check{\boldsymbol{G}}^{(r,1)}[i], \ldots, \check{\boldsymbol{G}}^{(r,N_t)}[i]\right]$, $\check{\boldsymbol{G}}[i] = \left[\check{\boldsymbol{G}}_T^{(1)T}[i], \ldots, \check{\boldsymbol{G}}_T^{(N_r)T}[i]\right]^T$, $\boldsymbol{x} = [\tilde{\boldsymbol{x}}^{(1)T}, \ldots, \tilde{\boldsymbol{x}}^{(N_t)T}]^T$, and $\boldsymbol{\xi}'[i] = [\boldsymbol{\xi}'^{(1)T}[i], \ldots, \boldsymbol{\xi}'^{(N_r)T}[i]]^T$, (43) can be rewritten to represent the received blocks at all receive antennas as

$$\boldsymbol{y}'[i] = \boldsymbol{G}[i]\boldsymbol{x} + \check{\boldsymbol{G}}[i]\boldsymbol{x}^* + \boldsymbol{\xi}'[i] \tag{44}$$

Hence,

$$\tilde{\boldsymbol{y}}'[i] = \begin{bmatrix} \boldsymbol{y}'[i] \\ \boldsymbol{y}'^*[i] \end{bmatrix} = \underbrace{\begin{bmatrix} \boldsymbol{G}[i] & \check{\boldsymbol{G}}[i] \\ \check{\boldsymbol{G}}[i]^* & \boldsymbol{G}[i]^* \end{bmatrix}}_{\tilde{\boldsymbol{G}}[i]} \underbrace{\begin{bmatrix} \boldsymbol{x} \\ \boldsymbol{x}^* \end{bmatrix}}_{\tilde{\boldsymbol{x}}} + \underbrace{\begin{bmatrix} \boldsymbol{\xi}'[i] \\ \boldsymbol{\xi}'^*[i] \end{bmatrix}}_{\tilde{\boldsymbol{\xi}}'[i]} \tag{45}$$

Using (45), the solution of (42) is given by

$$\boldsymbol{U}_{k,\,\text{MMSE}}[i] = \left(\tilde{\boldsymbol{F}}_k(\tilde{\boldsymbol{G}}[i]\boldsymbol{R}_{\tilde{\boldsymbol{x}}}\tilde{\boldsymbol{G}}^H[i] + \boldsymbol{R}_{\tilde{\boldsymbol{\xi}}'})\tilde{\boldsymbol{F}}_k^H\right)^{-1} \tilde{\boldsymbol{F}}_k\tilde{\boldsymbol{G}}[i]\boldsymbol{R}_{\tilde{\boldsymbol{x}}}\bar{\boldsymbol{E}}^{(k)T} \tag{46}$$

where $\boldsymbol{R}_{\tilde{x}} = \sigma_s^2\boldsymbol{I}_{(6N_tN)}$, $\boldsymbol{R}_{\tilde{\boldsymbol{\xi}}'}$ is obtained following the procedure used in the Appendix for $\boldsymbol{R}_{\tilde{\boldsymbol{\xi}}}$ and $\bar{\boldsymbol{E}}^{(k)} = \text{diag}\{[\boldsymbol{I}_{N_t} \otimes \bar{\boldsymbol{e}}^{(N+k)T}, \boldsymbol{I}_{N_t} \otimes \bar{\boldsymbol{e}}^{(2N-k)T}]\}$ where $\bar{\boldsymbol{e}}^{(N+k)}$ and $\bar{\boldsymbol{e}}^{(2N-k)}$ are the $(3N) \times 1$ unit vectors with a 1 in the positions $N + k$ and $2N - k$, respectively.

To compute $\boldsymbol{U}_{k,\,\text{MMSE}}[i]$ in (46), one sliding FFT per receive antenna is required. In the following, a low-complexity approach is derived which replaces each sliding FFT with only one full FFT and L' difference terms that are common to all subcarriers similar to the procedure in [30]. In (38), the term $\tilde{\boldsymbol{\mathcal{F}}}^{(k+q')}\boldsymbol{y}'^{(r)}[i]$ can be written as

$$\tilde{\mathcal{F}}^{(k+q')}\boldsymbol{y}'^{(r)}[i] = \boldsymbol{T}^{(k+q')}\begin{bmatrix} y^{(r)}_{f,\,k+q'}[i] \\ \Delta\boldsymbol{y}'^{(r)}[i] \end{bmatrix} \tag{47}$$

where $\boldsymbol{T}^{(k+q')}$ is an $(L'+1)\times(L'+1)$ lower triangular Toeplitz matrix given by

$$\boldsymbol{T}^{(k+q')} = \begin{bmatrix} 1 & 0 & \cdots & 0 \\ \vartheta^{(k+q')} & \ddots & \ddots & \vdots \\ \vdots & \ddots & \ddots & 0 \\ \vartheta^{(k+q')L'} & \cdots & \vartheta^{(k+q')} & 1 \end{bmatrix}$$

with $\vartheta = e^{-j2\pi/N}$, $y^{(r)}_{f,\,k+q'}[i]$ is the $(k+q')$th frequency component of the rth received signal, which is computed as $y^{(r)}_{f,\,k+q'}[i] = \mathcal{F}^{(k+q')}[y^{(r)}[i(N+c)+c+d+1], \ldots, y^{(r)}[(i+1)(N+c)+d]]^T$ and the difference terms $\Delta\boldsymbol{y}'^{(r)}[i]$ are given by $\Delta\boldsymbol{y}'^{(r)}[i] = [y^{(r)}[i(N+c)+c+d] - y^{(r)}[(i+1)(N+c)+d],\ \ldots,\ y^{(r)}[i(N+c)+c+d-L'+1] - y^{(r)}[(i+1)(N+c)+d-L'+1]]^T$.

Substituting (47) in (38) and defining $\boldsymbol{\varpi}^{(r,\,k)\,T}_{q'}[i] = \alpha^{(r,\,k)}_{q'}[i]\boldsymbol{\varrho}^{(r,\,k)\,T}_{q'}[i]\,\boldsymbol{T}^{(k+q')} = [\varpi^{(r,\,k)}_{q',0}[i], \ldots, \varpi^{(r,\,k)}_{q',L'}[i]]^T$, $\boldsymbol{\varsigma}^{(r,\,k)}_1[i] = [\varpi^{(r,\,k)}_{-Q'/2,0}[i], \ldots, \varpi^{(r,\,k)}_{Q'/2,0}[i]]^T$, $\boldsymbol{\varsigma}^{(r,\,k)}_2[i] = \left[\sum_{q'=-Q'/2}^{Q'/2}\varpi^{(r,\,k)}_{q',1}[i], \ldots, \sum_{q'=-Q'/2}^{Q'/2}\varpi^{(r,\,k)}_{q',L'}[i]\right]^T$ and $\boldsymbol{v}^{(r,\,k)\,T}_1 = [\boldsymbol{\varsigma}^{(r,\,k)\,T}_1[i], \boldsymbol{\varsigma}^{(r,\,k)\,T}_2[i]]$ results in

$$\hat{\tilde{y}}^{(r)}_{f,\,k}[i] = \boldsymbol{v}^{(r,\,k)T}_1[i] \times \underbrace{\begin{bmatrix} \boldsymbol{0}_{1\times L'} & & \mathcal{F}^{(k-Q'/2)} & \\ \vdots & & \vdots & \\ \boldsymbol{0}_{1\times L'} & & \mathcal{F}^{(k+Q'/2)} & \\ \bar{\boldsymbol{I}}_{L'} & \boldsymbol{0}_{L'\times(N-L')} & & -\bar{\boldsymbol{I}}_{L'} \end{bmatrix}}_{\bar{\boldsymbol{F}}^{(k)}} \boldsymbol{y}'^{(r)}[i] \tag{48}$$

where $\bar{\boldsymbol{I}}_{L'}$ is the anti-diagonal identity matrix of size $L'\times L'$.

Equation (48) is similar to (39), hence a similar approach is used to obtain the following design criterion:

$$\boldsymbol{\mathcal{V}}_{k,\,\mathrm{MMSE}}[i] = \arg\min_{\boldsymbol{\mathcal{V}}_k[i]}\ \mathcal{E}\left\{\left\|\tilde{\boldsymbol{x}}_k[i] - \boldsymbol{\mathcal{V}}^H_k[i]\bar{\boldsymbol{F}}_k\tilde{\boldsymbol{y}}'[i]\right\|^2\right\} \tag{49}$$

where $\bar{\boldsymbol{F}}_k = \mathrm{diag}\left\{\left[\boldsymbol{I}_{N_r}\otimes\bar{\boldsymbol{F}}^{(k)}, \boldsymbol{I}_{N_r}\otimes\bar{\boldsymbol{F}}^{(N-k)*}\right]\right\}$.

The solution of this MMSE problem is similar to (46) but it does not require any sliding FFT. The proposed low-complexity equalization and IQ imbalance compensation scheme in the presence of IBI/ICI is depicted in Fig. 5 for the kth subcarrier on the ath transmit antenna. This scheme is denoted by EQCS2. The design complexity of this scheme is of $\mathcal{O}(N_r(N+L')^2(Q'+L'+1))$ multiply-add (MA) operations per tone per transmit antenna. Also, its implementation complexity is $2N_r(Q'+L'+1)$ MA operations per tone per transmit antenna plus $\mathcal{O}(N_rN\log_2N)$ MA operations for the FFTs. It should be noted that the proposed scheme in Fig. 5 can be viewed as an extension of the proposed compensation methods in Sects. 3 and 4.1. It is also worth noting that this approach unifies and extends some existing methods for equalization and/or IQ imbalance compensation.

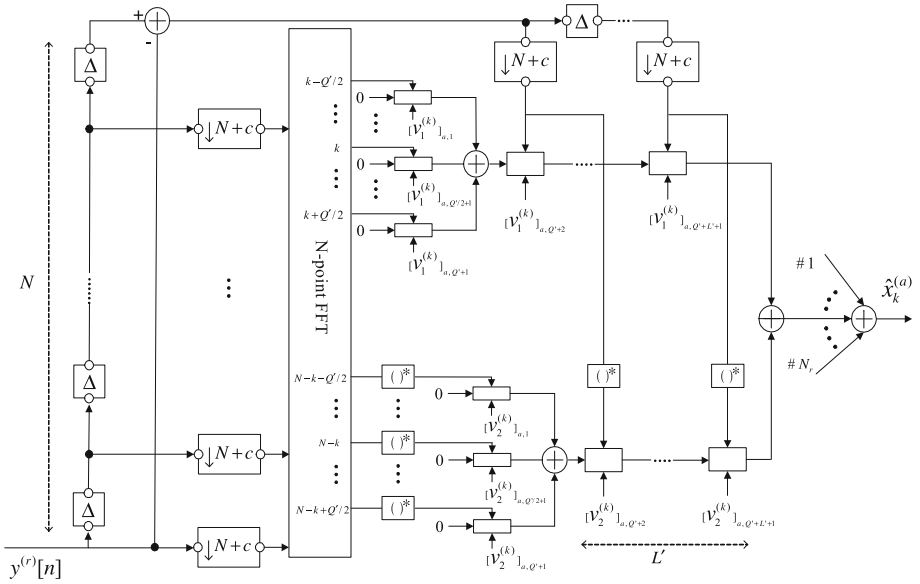

Fig. 5 Proposed equalization and IQ imbalance compensation scheme for insufficient CP (EQCS2)

(a) SISO-OFDM transmission over frequency selective channels

- In the presence of Rx FI IQ imbalance and IBI, the EQCS2 boils down to the per-tone equalizer (PTEQ) suggested in [31].
- In the presence of Rx FI IQ imbalance, IBI and CFO, the proposed equalizer in [31] is a special case of the EQCS2.
- In the presence of Tx/Rx IQ imbalance and IBI, the EQCS2 reduces to the frequency-domain equalizer proposed in [32].

(b) SISO-OFDM transmission over DS channels

- In the presence of Rx FI IQ imbalance, CFO and IBI, if critically-sampled CE-BEM ($K = N$) is used, the EQCS2 corresponds to the PTEQ proposed in [27].

(c) SIMO-OFDM transmission over DS channels

- When there is no IQ imbalance, if critically-sampled CE-BEM ($K = N$) is used, the EQCS2 reduces to the low-complexity PTEQ suggested in [33].

5 Simulations

In this section, the performance of the proposed equalization and compensation scheme for insufficient CP case (EQCS2) is evaluated for uncoded SISO-OFDM as well as MIMO-OFDM systems. The size of FFT is $N = 64$, the CP length is $c = 4$, and the signaling is 4-QPSK. The channel is of order $L = 3$. The channel taps are generated as i.i.d. random variables and correlated in time with a correlation function according to Jakes' model $\mathcal{E}\{g^{(r_1,t_1)}[n_1;l_1]g^{(r_2,t_2)*}[n_2;l_2]\} = \sigma_g^2 J_0(2\pi f_{\max} T(n_1-n_2))\delta[l_1-l_2]\delta[r_1-r_2]\delta[t_1-t_2]$, where J_0 is the zero-order Bessel function of the first kind and σ_g^2 denotes the variance of

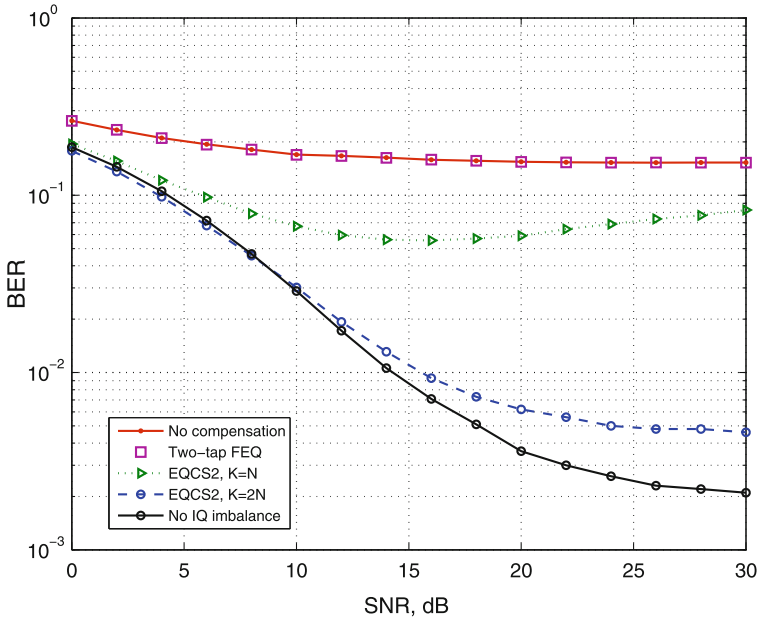

Fig. 6 BER comparison for SISO-OFDM system with IQ imbalance

the channel gain. The maximum Doppler spread is $f_{\max} = 180\,\text{Hz}$, the sampling time is $T = 50\,\mu\text{s}$, the number of TV basis functions in BEM is $Q = 4$, the number of adjacent neighbors is $Q' = 8$, $L' = 8$ and the decision delay is chosen to be $d = 1$. The performance is evaluated in terms of BER versus signal-to-noise-ratio (SNR). The SNR is defined as

$$\text{SNR} \triangleq (\max(L_1, L_2) + 1)\sigma_s^2 \,/\sigma_v^2$$

In the following, three simulation scenarios are considered. In the first scenario, a SISO-OFDM system is simulated. The FI amplitude imbalances are $\alpha_t = \alpha_r = 0.5\,\text{dB}$ and the phase imbalances are $\varphi_t = \varphi_r = 4°$. For FD IQ imbalance, the Tx/Rx front-end imbalance filters are $\zeta_t^I(t) = \zeta_r^I(t) = 0.04\delta(t) + \delta(t-T) + 0.01\delta(t-2T)$ and $\zeta_t^Q(t) = \zeta_r^Q(t) = 0.01\delta(t) + 1.2\delta(t-T) + 0.2\delta(t-2T)$. Figure 6 illustrates the simulation results for SISO-OFDM system. As a benchmark, the case of an ideal system with no IQ imbalance as well as a system with no compensation algorithm is also considered. The ideal system uses the PTEQ proposed in [34] to eliminate the IBI and ICI. The system with no IQ imbalance compensation scheme, only uses the one-tap FEQ [29] for channel compensation. Figure 6 shows that the IQ imbalance severely degrades the BER performance and the system with no compensation is unusable. It is also seen that the simple two-tap FEQ is incapable of compensating the IQ imbalance. The simulated two-tap FEQ is similar to the proposed approach in Sect. 3 and can be viewed as special case of the EQCS2, when $L' = Q' = 0$. As shown in Fig. 6, when critically-sampled CE-BEM, i.e. $K = N$, is used, the EQCS2 improves the simple two-tap FEQ, however, it shows an early error floor at BER = 5.56×10^{-2} (SNR = 16 dB). For over-sampled case, i.e. $K = 2N$, the EQCS2 provides good compensation performance which is close to the ideal case, especially for low to moderate SNR values.

In the second scenario, a MIMO-OFDM system with $N_t = 2$ transmit antennas and $N_r = 4$ receive antennas is simulated. It is assumed that the IQ imbalance parameters of each

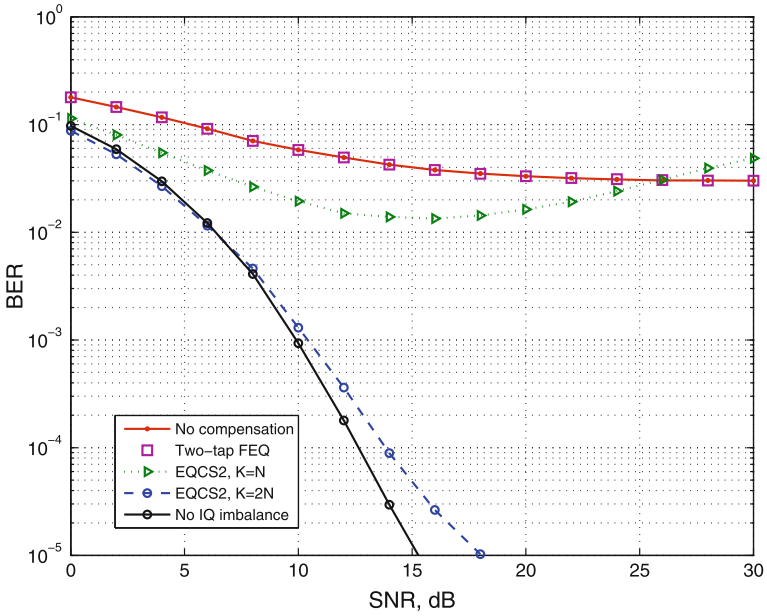

Fig. 7 BER comparison for MIMO-OFDM system with IQ imbalance (all transmit-receive branches have the same imbalance parameters)

transmit-receive antenna pair is the same as the imbalance parameters of the SISO case in the previous scenario. Figure 7 depicts the BER curves for MIMO-OFDM system. Again, the simple two-tap FEQ can not compensate for the IQ imbalance and has the same performance as the no compensation case. Also, the EQCS2 with critically-sampled CE-BEM has a poor performance and suffers from an early error floor. On the other hand, when $K = 2N$, the EQCS2 approaches the performance of the system with no IQ imbalance. Moreover, comparing Figs. 6 and 7 reveals that using the MIMO system significantly improves the BER performance over SISO case.

In the third scenario, a MIMO-OFDM system with $N_t = 2$ transmit antennas and $N_r = 4$ receive antennas is simulated again. However, in this scenario a different set of IQ imbalance parameters is used for each transmit-receive antenna pair. Table 1 gives the imbalance parameters. Figure 8 shows the simulation result of this scenario. It is evident that the BER curves in Figs. 7 and 8 are similar. Therefore, the performance of the EQCS2 is robust with respect to the changes in the IQ imbalance parameters of different transmit-receive branches.

6 Conclusion

The paper addressed the joint effects of both transmitter and receiver FI/FD IQ imbalance in MIMO-OFDM transmission over doubly selective channels. Using CE-BEM, an input-output relation is developed as a function of both Tx/Rx imbalance parameters and TV channel impulse response. This relation is then deployed to derive two digital-domain joint IBI/ICI equalization and FI/FD IQ imbalance compensation methods for the cases of sufficient or insufficient CPs. These methods are designed and realized in the frequency domain for each subcarrier, separately.

Table 1 IQ imbalance parameters for third simulation scenario

	α_t (dB)	φ_t (deg.)	ξ_t^I	ξ_t^Q
Transmitter side				
Tx1	0.7	2	[0.02 0.9 0.01]	[0.1 1.2 0.02]
Tx2	0.4	5	[0.01 1.1 0.02]	[0.02 1 0.01]
	α_r (dB)	φ_r (deg.)	ξ_r^I	ξ_r^Q
Receiver side				
Rx1	0.1	7	[0.01 0.8 0.1]	[0.02 1.1 0.01]
Rx2	0.4	3	[0.03 1.1 0.01]	[0.01 1 0.2]
Rx3	0.7	2	[0.03 1 0.02]	[0.02 1.3 0.2]
Rx4	0.6	6	[0.02 0.7 0.01]	[0.01 1 0.03]

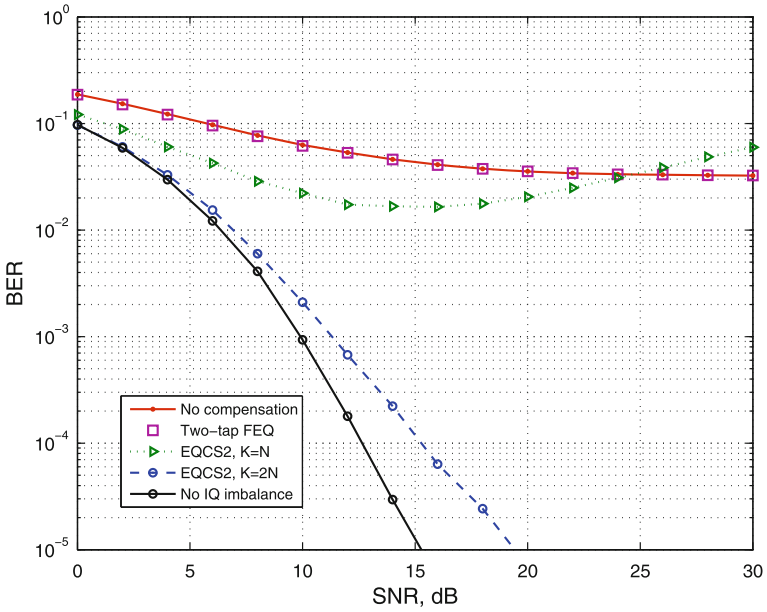

Fig. 8 BER comparison for MIMO-OFDM system with IQ imbalance (different transmit-receive branches have different imbalance parameters)

Simulation results show that the IQ imbalance can severely limit the achievable BER. So, efficient imbalance compensation is crucial. It is seen that the proposed method for insufficient CP case (EQCS2) achieves a BER performance that is near to the performance of a system with ideal IQ branches in both SISO- and MIMO-OFDM systems. In addition, using the MIMO system, significantly improves the BER performance over SISO case.

Appendix

In this Appendix, an expression for computing the noise correlation matrix $\boldsymbol{R}_{\tilde{\boldsymbol{\xi}}}$ in (24) is derived. The noise term $\xi^{(r)}[n]$ in (11) can be expressed as

$$\xi^{(r)}[n] = \eta^{(r)}[n] + \breve{\eta}^{(r)}[n] = \lambda_r^{(r)}[n] \star \upsilon^{(r)}[n] + \phi_r^{(r)}[n] \star \upsilon^{(r)*}[n] \tag{50}$$

Using (50), the noise vector of length N at the rth receive antenna is given by

$$\boldsymbol{\xi}^{(r)}[i] = \boldsymbol{\Lambda}_r^{(r)} \boldsymbol{\upsilon}^{(r)}[i] + \boldsymbol{\Phi}_r^{(r)} \boldsymbol{\upsilon}^{(r)*}[i] = \boldsymbol{\Lambda}_r^{(r)} \boldsymbol{\upsilon}^{(r)}[i] + \boldsymbol{\Phi}_r^{(r)} \boldsymbol{\upsilon}^{(r)*}[i] \tag{51}$$

where $\boldsymbol{\upsilon}^{(r)}[i] = [\upsilon^{(r)}[i(N+c)+c+d-L_{\lambda_r}+1], \ldots, \upsilon^{(r)}[(i+1)(N+c)+d]]^T$, $\boldsymbol{\Lambda}_r^{(r)}$ is an $N \times (N + L_{\lambda_r})$ Toeplitz matrix with the $\jmath$th row as $[\mathbf{0}_{1\times(\jmath-1)}, \lambda_{r,L_{\lambda_r}}^{(r)}, \ldots, \lambda_{r,0}^{(r)}, \mathbf{0}_{1\times(N-\jmath)}]$ where $\lambda_{r,\ell}^{(r)}$ and L_{λ_r} are the ℓth coefficient and the order of $\lambda_r^{(r)}(t)$, respectively and $\boldsymbol{\Phi}_r^{(r)}$ is defined similar to $\boldsymbol{\Lambda}_r^{(r)}$.

Considering the noise vectors at all receive antennas yields

$$\boldsymbol{\xi}[i] = \boldsymbol{\Lambda}_r \boldsymbol{\upsilon}[i] + \boldsymbol{\Phi}_r \boldsymbol{\upsilon}^*[i] \tag{52}$$

where $\boldsymbol{\xi}[i] = [\boldsymbol{\xi}^{(1)\,T}[i], \ldots, \boldsymbol{\xi}^{(N_r)\,T}[i]]^T$, $\boldsymbol{\Lambda}_r = \text{diag}\{[\boldsymbol{\Lambda}_r^{(1)}, \ldots, \boldsymbol{\Lambda}_r^{(N_r)}]\}$, $\boldsymbol{\Phi}_r = \text{diag}\{[\boldsymbol{\Phi}_r^{(1)}, \ldots, \boldsymbol{\Phi}_r^{(N_r)}]\}$ and $\boldsymbol{\upsilon}[i] = [\boldsymbol{\upsilon}^{(1)\,T}[i], \ldots, \boldsymbol{\upsilon}^{(N_r)\,T}[i]]^T$. Therefore, the noise term $\tilde{\boldsymbol{\xi}}[i]$ is written as

$$\tilde{\boldsymbol{\xi}}[i] = \begin{bmatrix} \boldsymbol{\xi}[i] \\ \boldsymbol{\xi}^*[i] \end{bmatrix} = \underbrace{\begin{bmatrix} \boldsymbol{\Lambda}_r & \boldsymbol{\Phi}_r \\ \boldsymbol{\Phi}_r^* & \boldsymbol{\Lambda}_r^* \end{bmatrix}}_{\boldsymbol{A}} \begin{bmatrix} \boldsymbol{\upsilon}[i] \\ \boldsymbol{\upsilon}^*[i] \end{bmatrix} \tag{53}$$

Finally, the correlation matrix $\boldsymbol{R}_{\tilde{\boldsymbol{\xi}}}$ is obtained as

$$\boldsymbol{R}_{\tilde{\boldsymbol{\xi}}} = \mathcal{E}\{\tilde{\boldsymbol{\xi}}[i]\tilde{\boldsymbol{\xi}}^H[i]\} = \sigma_\upsilon^2 \boldsymbol{A}\boldsymbol{A}^H \tag{54}$$

References

1. Weinstein, S., & Ebert, P. (1971). Data transmission by frequency-division multiplexing using the discrete Fourier transform. *IEEE Transactions on Communication Technology, 19*(5), 628–634.
2. Li, Y. G., & Stuber, G. L. (2009). *Orthogonal frequency division multiplexing for wireless communications*. Atlanta, GA: Springer.
3. Fazel, Kh., & Kaiser, S. (2008). *Multi-carrier and spread spectrum systems: From OFDM and MC-CDMA to LTE and WiMAX*. UK: Wiley.
4. Hwang, T., Yang, Ch., Wu, G., Li, Sh., & Li, G. Y. (2009). OFDM and its wireless applications: A survey. *IEEE Transactions on Vehicular Technology, 58*(4), 1673–1694.
5. Hanzo, L., Akhtman, Y., Wang, L., & Jiang, M. (2011). *MIMO-OFDM for LTE, WiFi and WiMAX: Coherent versus non-coherent and cooperative turbo transceivers*. UK: Wiley.
6. Fettweis, G., Löhning, M., Petrovic, D., Windisch, M., Zillmann, P., & Rave, W. (2007). Dirty RF: A new paradigm. *International Journal of Wireless Information Networks, 14*(2), 133–148.
7. Schenk, T. C. W. (2008). *RF imperfections in high-rate wireless systems: Impact and digital compensation*. Netherlands: Springer.
8. Valkama, M., Springer, A., & Hueber, G. (2010). Digital signal processing for reducing the effects of RF imperfections in radio devices—an overview. In *Proceedings of IEEE international symposiom on circuits and systems* (pp. 813–816.) Paris, France.
9. Razavi, B. (1998). *RF microelectronics*. Upper Saddle River, NJ: Prentice Hall.
10. Abidi, A. (1995). Direct-conversion radio transceivers for digital communications. *IEEE Journal of Solid-State Circuits, 30*(12), 1399–1410.

11. Liu, C. L. (1998). Impacts of I/Q imbalance on QPSK-OFDM-QAM detection. *IEEE Transactions on Consumer Electronics, 44*(3), 984–989.
12. Schuchert, A., Hasholzner, R., & Antoine, P. (2001). A novel IQ imbalance compensation scheme for the reception of OFDM signals. *IEEE Transactions on Consummer Electronics, 47*(3), 313–318.
13. Tarighat, A., & Sayed, A. H. (2007). Joint compensation of transmitter and receiver impairments in OFDM systems. *IEEE Transactions on Wireless Communications, 6*(1), 240–247.
14. Tandur, D., & Moonen, M. (2007). Joint adaptive compensation of transmitter and receiver IQ imbalance under carrier frequency offset in OFDM-based systems. *IEEE Transactions on Signal Processing, 55*(11), 5246–5252.
15. Feigin, J., & Brady, D. (2009). Joint transmitter/receiver I/Q imbalance compensation for direct conversion OFDM in packet-switched multipath environments. *IEEE Transactions on Signal Processing, 57*(11), 4588–4593.
16. Krondorf, M., & Fettweis, G. (2008). OFDM link performance analysis under various receiver impairments. *EURASIP Journal of Wireless Communications and Networking*. doi:10.1155/2008/145279.
17. Jin, Y., Kwon, J., Lee, Y., Lee, D., & Ahn, J. (2008). Obtained diversity gain in OFDM systems under the influence of IQ imbalance. *IEICE Transactions on Communications, 91-B*(3), 814–820.
18. Park, J., Lee, Y., & Park, H. (2009). Preamble design for joint estimation of CFO and I/Q imbalance for direct conversion OFDM system. *IET Communications, 3*(4), 597–602.
19. Rao, R. M., & Daneshrad, B. (2004). IQ mismatch cancellation for MIMO-OFDM systems. In *Proceedings of IEEE international symposiom on personal, indoor, and mobile radio communications* (pp. 2710–2714). Barcelona, Spain.
20. Schenk, T. C. W. (2007). Performance analysis of zero-IF MIMO OFDM transceivers with IQ imbalance. *Journal of Communications, 2*(7), 9–19.
21. Tarighat, A., & Sayed, A. H. (2005). MIMO OFDM receivers for systems with IQ imbalances. *IEEE Transactions on Signal Processing, 53*(9), 3583–3596.
22. Rao, R. M., & Daneshrad, B. (2006). Analog impairments in MIMO-OFDM systems. *IEEE Transactions on Wireless Communications, 5*(12), 3382–3387.
23. Zou, Y., Valkama, M., & Renfors, M. (2008). Digital compensation of I/Q imbalance effects in space-time coded transmit diversity systems. *IEEE Transactions on Signal Processing, 56*(6), 2496–2508.
24. Gao, J., Zhu, X., Lin, H., & Nandi, A. K. (2010). Independent component analysis based semi-blind I/Q imbalance compensation for MIMO-OFDM systems. *IEEE Transactions on Wireless Communications, 9*(3), 914–920.
25. Tsatsanis, M. K., & Giannakis, G. B. (1996). Modeling and equalization of rapidly fading channels. *International Journal of Adaptive Control and Signal Processing, 10*(2/3), 159–176.
26. Narasimhan, B., Wang, D., Narayanan, S., Minn, H., & Al-Dhahir, N. (2009). Digital compensation of frequency-dependent joint Tx/Rx I/Q imbalance in OFDM systems under high mobility. *IEEE Journal of Selected Topics on Signal Processing, 3*(3), 405–417.
27. Barhumi, I., & Moonen, M. (2006). Frequency domain IQ imbalance and carrier frequency offset compensation for OFDM over doubly selective channels. In *Proceedings of European signal processing conference* (pp. 3097–3100). Florence, Italy.
28. Leus, G., Zhou, S., & Giannakis, G. B. (2003). Orthogonal multiple access over time- and frequency-selective fading. *IEEE Transactions on Information Theory, 49*(8), 1942–1950.
29. Cai, X. D., & Giannakis, G. B. (2003). Bounding performance and suppressing intercarrier interfenence in wireless mobile OFDM. *IEEE Transactions on Communications, 51*(12), 2047–2056.
30. Farhang-Boroujeny, B., & Gazor, S. (1994). Generalized sliding FFT and its application to implementation of block LMS adaptive filters. *IEEE Transactions on Signal Processing, 42*(3), 532–538.
31. Barhumi, I., & Moonen, M. (2007). IQ-imbalance compensation for OFDM in the presence of IBI and carrier-frequency offset. *IEEE Transactions on Signal Processing, 55*(1), 256–266.
32. Tandur, D., & Moonen, M. (2007). Joint compensation of OFDM frequency selective transmitter and receiver IQ imbalance. *EURASIP Journal of Wireless Communications and Networking*. doi:10.1155/2007/68563.
33. Barhumi, I., Leus, G., & Moonen, M. (2006). Equalization for OFDM over doubly selective channels. *IEEE Transactions on Signal Processing, 54*(4), 1445–1458.
34. Beheshti, M., Omidi, M. J., & Doost-Hoseini, A. M. (2009). Equalization of SIMO-OFDM systems with insufficient cyclic prefix in doubly selective channels. *IET Communications, 3*(12), 1870–1882.

Author Biographies

Mojtaba Beheshti received the B.Sc. degree from the Isfahan University of Technology (IUT), Iran, the M.Sc. degree from the University of Tehran, and the Ph.D. degree from IUT in 1996, 1999, and 2011 respectively, all in electrical engineering. From 2001–2004, he worked as a researcher in the Electrical & Computer Engineering research center of IUT. Currently he is an assistant professor with the Information and Communication Technology Institute of IUT. His research interests include: signal processing for digital communications, multicarrier and MIMO systems and underwater acoustic communications.

Mohammad Javad Omidi received his Ph.D. from University of Toronto in 1998. He worked in industry by joining a research and development group designing broadband communication systems for 5 years. In 2003 he joined the Department of Electrical and Computer Engineering, at Isfahan University of Technology, Iran; and then served as the chair of Information Technology Center and ECE department at this university. His research interests are in the areas of mobile computing, wireless communications, digital communication systems, cognitive radio, and VLSI architectures for communication algorithms.

Ali Mohammad Doost-Hoseini received a B.Sc. degree in electrical engineering from Shiraz University, Iran, in 1975. M.Sc. and Ph.D. degrees were conferred to him, in the same field, by the University of California at Berkeley and Stanford University in 1978 and 1982, respectively. He joined Isfahan University of Technology in 1983 where he is currently an associate professor in the Electrical and Computer Engineering Department. He has taught numerous undergraduate and graduate courses in EE, and supervised several M.Sc. and Ph.D. dissertations, mainly, in the fields of estimation and digital communications.